to remove nonspecific bound protein. Then, samples were incubated with primary antibody at 4°C for 2 h followed by incubation with protein G–Sepharose beads. Lysates and immunoprecipitates were resolved by SDS-PAGE and transferred to a polyvinylidene difluoride membrane (GE Healthcare). The membrane was preblotted in milk buffer for 1 h and immunoblotted with primary antibody for 2 h. HRP-conjugated secondary antibodies (Jackson ImmunoResearch Laboratories) were used, and proteins were visualized using an enhanced chemiluminescence substrate kit (GE Healthcare).

2-deoxyglucose uptake

Differentiated adipocytes were prepared in 24-well plates. Cells were infected with the recombinant adenoviruses. 2 d thereafter, the cells were serum starved for 2 h at 37°C in Krebs-Ringer phosphate buffer (130 mM NaCl, 5 mM KCl, 1.3 mM $CaCl_2$, 1.3 mM $MgSO_4$, and 10 mM Na_2HPO_4, pH 7.4) and were treated with or without 20 ng/ml TNF-α for 4 h. Next, the cells were stimulated with or without 100 nM insulin for 5 min, and 2-deoxyglucose uptake was determined by 2-deoxy-D-[2,6 ^{3}H] glucose incorporation. Nonspecific deoxyglucose uptake was measured in the presence of 20 μM cytochalasin B and subtracted from each determination to obtain specific uptake. The deoxyglucose uptake was corrected using the protein amount.

In vitro kinase assay

3T3-L1 adipocytes were infected with the recombinant adenoviruses as indicated. 2 d after the infection, cells were stimulated with or without 20 ng/ml TNF-α for 5 min, and cell lysates were prepared. After adjusting the protein concentration, immunoprecipitation using anti–IKK-β antibody was performed. Precipitates were mixed with IKK substrate peptide (KKKKERLLDDRHDSGLDSMKDEE; Upstate Biotechnology) and γ-[^{32}P] ATP. After a 10-min incubation at 30°C, samples were transferred to P81 paper (Whatman) and washed with 0.75% phosphoric acid and acetone. Radioactivity was counted using a scintillation counter.

Statistical analysis

Multiple comparisons among groups were performed using the one-factor analysis of variance test (post-hoc test; Turkey-Kramer). Results are presented as means ± SD. Values of $P < 0.05$ were considered statistically significant.

Online supplemental material

Fig. S1 shows the results of pull-down experiments to demonstrate the direct interaction of NEMO with Myo1c. Fig. S2 shows the effects of NEMO knockdown on Myo1c–IKK-β interaction (A) and the effects of NEMO expression on IRS-1–IKK-β interaction (B). Fig. S3 shows the effects of Myo1c expression on the TNF-α–induced phosphorylation of IRS-1 Ser^{307} (A) and the effects of WT NEMO and ΔN-NEMO expression or NEMO knockdown on IKK-β kinase activity (B and C). Online supplemental material is available at http://www.jcb.org/cgi/content/full/jcb.200601065/DC1.

We thank Dr. Hiroyasu Nakano for providing the IKK-α and -β constructs. We are also grateful to Dr. Teruo Nishida (Yamaguchi University Graduate School of Medicine, Yamaguchi, Japan) for allowing us to use his confocal microscope.

This work was partly supported by Grants-in-Aid for Scientific Research (KAKENHI) from the Ministry of Education, Culture, Sports, Science and Technology of Japan (15590940 and 17590934) to M. Emoto and the Research Grant for Longevity Sciences from the Ministry of Health, Labor, and Welfare of Japan (15C-8) to Y. Tanizawa.

Submitted: 12 January 2006
Accepted: 1 May 2006

References

Bose, A., A. Guilherme, S.I. Robida, S.M. Nicoloro, Q.L. Zhou, Z.Y. Jiang, D.P. Pomerleau, and M.P. Czech. 2002. Glucose transporter recycling in response to insulin is facilitated by myosin Myo1c. *Nature*. 420:821–824.

de Alvaro, C., T. Teruel, R. Hernandez, and M. Lorenzo. 2004. Tumor necrosis factor α produces insulin resistance in skeletal muscle by activation of inhibitor κB kinase in a p38 MAPK-dependent manner. *J. Biol. Chem.* 279:17070–17078.

DiDonato, J.A., M. Hayakawa, D.M. Rothwarf, E. Zandi, and M. Karin. 1997. A cytokine-responsive IκB kinase that activates the transcription factor NF-κB. *Nature*. 388:548–554.

Dorner, C., A. Ullrich, H.U. Haring, and R. Lammers. 1999. The kinesin-like motor protein KIF1C occurs in intact cells as a dimer and associates with proteins of the 14-3-3 family. *J. Biol. Chem.* 274:33654–33660.

Emoto, M., S.E. Langille, and M.P. Czech. 2001. A role for kinesin in insulin-stimulated GLUT4 glucose transporter translocation in 3T3-L1 adipocytes. *J. Biol. Chem.* 276:10677–10682.

Gao, Z., D. Hwang, F. Bataille, M. Lefevre, D. York, M.J. Quon, and J. Ye. 2002. Serine phosphorylation of insulin receptor substrate 1 by inhibitor κB kinase complex. *J. Biol. Chem.* 277:48115–48121.

Hotamisligil, G.S., N.S. Shargill, and B.M. Spiegelman. 1993. Adipose expression of tumor necrosis factor-α: direct role in obesity-linked insulin resistance. *Science*. 259:87–91.

Kanety, H., R. Feinstein, M.Z. Papa, R. Hemi, and A. Karasik. 1995. Tumor necrosis factor α-induced phosphorylation of insulin receptor substrate-1 (IRS-1). Possible mechanism for suppression of insulin-stimulated tyrosine phosphorylation of IRS-1. *J. Biol. Chem.* 270:23780–23784.

Kim, J.K., Y.J. Kim, J.J. Fillmore, Y. Chen, I. Moore, J. Lee, M. Yuan, Z.W. Li, M. Karin, P. Perret, et al. 2001. Prevention of fat-induced insulin resistance by salicylate. *J. Clin. Invest.* 108:437–446.

Luo, J., S.J. Field, J.Y. Lee, J.A. Engelman, and L.C. Cantley. 2005. The p85 regulatory subunit of phosphoinositide 3-kinase down-regulates IRS-1 signaling via the formation of a sequestration complex. *J. Cell Biol.* 170:455–464.

Miyagishi, M., and K. Taira. 2002. U6 promoter-driven siRNAs with four uridine 3′ overhangs efficiently suppress targeted gene expression in mammalian cells. *Nat. Biotechnol.* 20:497–500.

Nakano, H., M. Shindo, S. Sakon, S. Nishinaka, M. Mihara, H. Yagita, and K. Okumura. 1998. Differential regulation of IκB kinase α and β by two upstream kinases, NF-κB–inducing kinase and mitogen-activated protein kinase/ERK kinase kinase-1. *Proc. Natl. Acad. Sci. USA*. 95:3537–3542.

Reaven, G.M. 1988. Banting lecture 1988. Role of insulin resistance in human disease. *Diabetes*. 37:1595–1607.

Setou, M., T. Nakagawa, D.H. Seog, and N. Hirokawa. 2000. Kinesin superfamily motor protein KIF17 and mLin-10 in NMDA receptor-containing vesicle transport. *Science*. 288:1796–1802.

Shevchenko, A., M. Wilm, O. Vorm, and M. Mann. 1996. Mass spectrometric sequencing of proteins from silver-stained polyacrylamide gels. *Anal. Chem.* 68:850–858.

Weil, R., K. Schwamborn, A. Alcover, C. Bessia, V. Di Bartolo, and A. Israel. 2003. Induction of the NF-κB cascade by recruitment of the scaffold molecule NEMO to the T cell receptor. *Immunity*. 18:13–26.

Williamson, R.T., and M.D. Lond. 1901. On the treatment of glycosuria and diabetes mellitus with sodium salicylate. *Brit. Med. J.* 1:760–762.

Yamamoto, Y., D.W. Kim, Y.T. Kwak, S. Prajapati, U. Verma, and R.B. Gaynor. 2001. IKKγ /NEMO facilitates the recruitment of the IκB proteins into the IκB kinase complex. *J. Biol. Chem.* 276:36327–36336.

Yamaoka, S., G. Courtois, C. Bessia, S.T. Whiteside, R. Weil, F. Agou, H.E. Kirk, R.J. Kay, and A. Israel. 1998. Complementation cloning of NEMO, a component of the IκB kinase complex essential for NF-κB activation. *Cell*. 93:1231–1240.

Yin, M.J., Y. Yamamoto, and R.B. Gaynor. 1998. The anti-inflammatory agents aspirin and salicylate inhibit the activity of IκB kinase-β. *Nature*. 396:77–80.

Yuan, M., N. Konstantopoulos, J. Lee, L. Hansen, Z.W. Li, M. Karin, and S.E. Shoelson. 2001. Reversal of obesity- and diet-induced insulin resistance with salicylates or targeted disruption of Ikkβ. *Science*. 293:1673–1677.

Gene Therapy (2006) 13, 883–892

www.nature.com/gt

ORIGINAL ARTICLE

Intracellular-diced dsRNA has enhanced efficacy for silencing HCV RNA and overcomes variation in the viral genotype

T Watanabe[1,4], M Sudoh[2], M Miyagishi[3], H Akashi[3], M Arai[1,5], K Inoue[1,4], K Taira[3], M Yoshiba[4] and M Kohara[1]

[1]Department of Microbiology and Cell Biology, The Tokyo Metropolitan Institute of Medical Science, Tokyo, Japan; [2]Kamakura Research Labs, Chugai Pharmaceutical Co. Ltd, Kanagawa, Japan; [3]Department of Chemistry and Biotechnology, School of Engineering, The University of Tokyo, Tokyo, Japan; [4]Division of Gastroenterology, Showa University Fujigaoka Hospital, Yokohama, Japan and [5]Research & Development Division, Mitsubishi Pharma Corporation, Yokohama, Japan

RNA interference (RNAi) can be used to inhibit viral replication in mammalian cells and therefore could be a powerful new antiviral therapy. Small interfering RNA (siRNA) may be effective for RNAi, but there are some technical problems that must be solved in each case, for example, predicting the effective siRNA target site and targeting heterogeneous sequences in a virus population. We show here that diced siRNA generated from long double-stranded RNA (dsRNA) is highly effective for inducing RNAi in HuH-7 cells harboring hepatitis C virus (HCV) replicons and can overcome variations in the HCV genotype. However, in mammalian cells, long dsRNA induced an interferon response and caused cell death. Here we describe an improvement of this method, U6 promoter-driven expression of long hairpin-RNA with multiple point mutations in the sense strand. This can efficiently silence HCV RNA replication and HCV protein expression without triggering the interferon response or cell death normally caused by dsRNA. In conclusion, intracellular-diced dsRNA efficiently induces RNAi, and, despite the high rate of mutation in HCV, it should be a feasible therapeutic strategy for silencing HCV RNA.

Gene Therapy (2006) **13**, 883–892. doi:10.1038/sj.gt.3302734; published online 23 February 2006

Keywords: *RNAi; long dsRNA; dicer; heterogeneous; interferon; U6 vector; HCV*

Introduction

An estimated 170 million people worldwide are persistently infected with hepatitis C virus (HCV).[1] Although the initial infection is frequently asymptomatic, there are several subsequent clinical manifestations, including fibrosis of the liver, cirrhosis and hepatocellular carcinoma. Although combination therapy with interferon (IFN)-α and ribavirin has markedly improved the clinical outcome, less than half of the patients with chronic hepatitis C can be expected to respond favorably to currently available agents.[2] Therefore, developing a new therapy for chronic HCV is a major public health objective.

The genome of HCV, a member of Flaviviridae family, is encoded in an approximately 9.6-kb single-stranded RNA with positive polarity that includes a 5′-untranslated region (UTR)[3] and a 3′-UTR containing a 3′X terminal sequence.[4] Hepatitis C virus displays a high rate of mutation and is classified into distinct genotypes (1–6) and subtypes, whose distribution varies both geographically and between risk groups.[5] Furthermore, several distinct but closely related HCV sequences coexist within each infected individual. These are referred to as quasispecies and reflect the high replication rate of the virus and the lack of a proofreading activity of the RNA-dependent RNA polymerase.[6,7]

Gene targeting with functional nucleic acids is commonly used to determine gene function and has potential as a treatment for viral diseases. Although antisense RNA and ribozyme technologies are successful in some situations, they have been difficult to apply universally and are less effective *in vivo*.[8] A possible alternative, sequence-specific post-transcriptional gene silencing by double-stranded RNA (dsRNA), also known as RNA interference (RNAi), has been found in plants, *Caenorhabditis elegans* and mammalian cells.[9,10] As RNAi with small interfering RNA (siRNA) can inhibit the replication of several viruses, including human immunodeficiency virus type 1 (HIV-1)[11] and poliovirus,[12] it may be a powerful new antiviral therapy. Recently, it has been demonstrated that replication of HCV RNA is also receptive to RNAi machinery,[13–18] but it has been difficult to design highly effective siRNAs against HCV because of the exquisite sequence specificity of the siRNAs coupled with the variation in HCV genotypes and the enormous diversity of HCV sequences between and within infected individuals.

Correspondence: Dr M Kohara, Department of Microbiology and Cell Biology, The Tokyo Metropolitan Institute of Medical Science, 3-18-22, Honkomagome, Bunkyo-ku, Tokyo 113-8613, Japan.
E-mail: mkohara@rinshoken.or.jp
Received 15 July 2005; revised 13 October 2005; accepted 1 November 2005; published online 23 February 2006

In this report, we show that dicer-generated siRNAs from long dsRNA can silence the replication of HCV RNA of different genotypes. Furthermore, we employed the modified long hairpin-RNA (hRNA) expression system to inhibit HCV replication and to avoid triggering the IFN response, which is normally caused by dsRNA. We demonstrated that intracellular-diced dsRNA can be used in mammalian cells to silence HCV RNA and, therefore, that long dsRNA-mediated RNAi could be useful as a therapeutic agent for natural viral infection by HCV.

Results

Synthetic small interfering RNA inhibits hepatitis C virus replication in HuH-7 cells containing replicating hepatitis C virus RNA

As siRNA-mediated RNAi is strictly sequence specific, an siRNA targeting site was selected in regions conserved among the various HCV genotypes. Of the HCV genome sequences, the 5′-UTR and the 3′X region are the most highly conserved.[19] Therefore, we selected six sites in the 5′-UTR or core coding regions (A–F) and three sites in the 3′X regions (G–I) (see Materials and methods). HuH-7 cells carrying the HCV replicon were established as described.[20] We also modified the replicon RNA derived from the HCV genotype 1b clone (GenBank accession number AY045702) by substituting the *neo*^{r} gene with the firefly luciferase gene fused to foot-and-mouth disease virus (FMDV) 2A and the *neo*^{r} gene (named the R6FLR-N replicon). This modification enables the sensitive and precise quantification of HCV replication levels using a luciferase assay.

To examine the ability of siRNAs to inhibit HCV replication, the nine synthetic siRNAs were transfected into R6FLR-N replicon cells (Figure 1a, left). Of the siRNAs, siE (nucleotides (nt) 325–344) was the most effective and it dose-dependently inhibited HCV replication (Figure 1a, right). Moreover, continuous transfection with siE but not the negative control p53m siRNA caused a gradual decrease in the HCV replicon titer up to the 23rd day (Figure 1b). Using Northern blot analysis, we confirmed that the effects of siRNAs on the luciferase activity are associated with siRNA-directed degradation of the HCV replicon RNA (data not shown). These results indicated that siE was the most potent siRNA for inhibiting HCV replication of the selected siRNA sites.

Effect of ex-vivo *dicer-generated small interfering RNAs from long double-stranded RNA*

We found that shifting the siRNAs 5′ or 3′ from the siE target position reduced the efficacy of siRNA-mediated RNAi (Figure 2a). Therefore, to overcome site specificity of the selected siRNAs, we prepared *ex-vivo* recombinant human dicer (rhDicer)-generated siRNAs (d-siRNAs) from long dsRNAs (Figure 2b).[21] R6FLR-N replicon cells were transfected with d-siRNAs targeting the HCV genome or p53 mRNA (negative control). Luciferase reporter assays indicated that d-siRNAs generated from the 5′-UTR of HCR6 sequences (D5-357, D5-197, and D5-50) silenced the HCV RNA more efficiently than siE. In contrast, the d-siRNAs generated from the 3′-UTR of the HCR6 sequences were less effective than siE. These

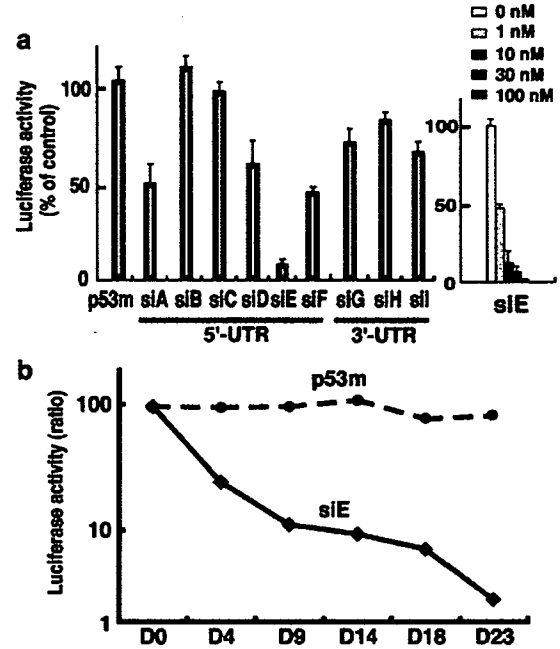

Figure 1 Effect of siRNA on HCV replication. (**a**) Inhibition of the HCV replicon by siRNAs in R6FLR-N replicon cells. Luciferase activity was measured 24 h after transfection using the Trans IT TKO reagent. Data represent means ± s.d. ($n = 3$) compared with mock-transfected cells. siA to siF, siRNA in the 5′-UTR or core cording regions; siG to siI, siRNA in the 3′-UTR; p53 m, negative control siRNA. (**b**) Long-term effect of siE. The R6FLR-N replicon cells were transfected with siRNAs every 4 days. Luciferase activity was measured on the indicated days.

results indicated that d-siRNAs generated from 5′-UTR containing the siE sequences, especially those generated from 197-bp dsRNAs, were more effective than the synthetic siE.

Dicer-generated siRNAs generated from 197-bp double-stranded RNA overcome hepatitis C virus genotype variation

Genotype 1b-derived d-siRNAs generated from the conserved sequence motifs within the NS5B sequence do not block the replication of HCV genotypes 1a and 2a.[14] To examine whether our selected d-siRNAs can overcome HCV genotype variation, we transfected genotype 2a-specific d-siRNAs into R6FLR-N replicon cells, which harbor the genotype 1b replicon. As shown in Figures 3a and b, the genotype 2a-derived d-siRNAs generated from 197-bp dsRNA efficiently inhibited genotype 1b replication, even though genotypes 2a and 1b differ by 15 bases within the 197-bp dsRNA sequences (sequence homology = 92%). In contrast, genotype 2a-derived siE, which harbors a single mutation at position 18 of the sense strand (sequence homology = 95%), showed a weak silencing activity against genotype 1b. These results demonstrated that d-siRNAs generated from the 197-bp dsRNA were highly effective for RNAi and could overcome HCV genotype variation.

Long double-stranded RNA transfection into HuH-7 replicon cells induces target-specific silencing

Dicer is a large multi-domain protein present in all eukaryotes.[22] Recently, Kim *et al*.[23] reported that syn-

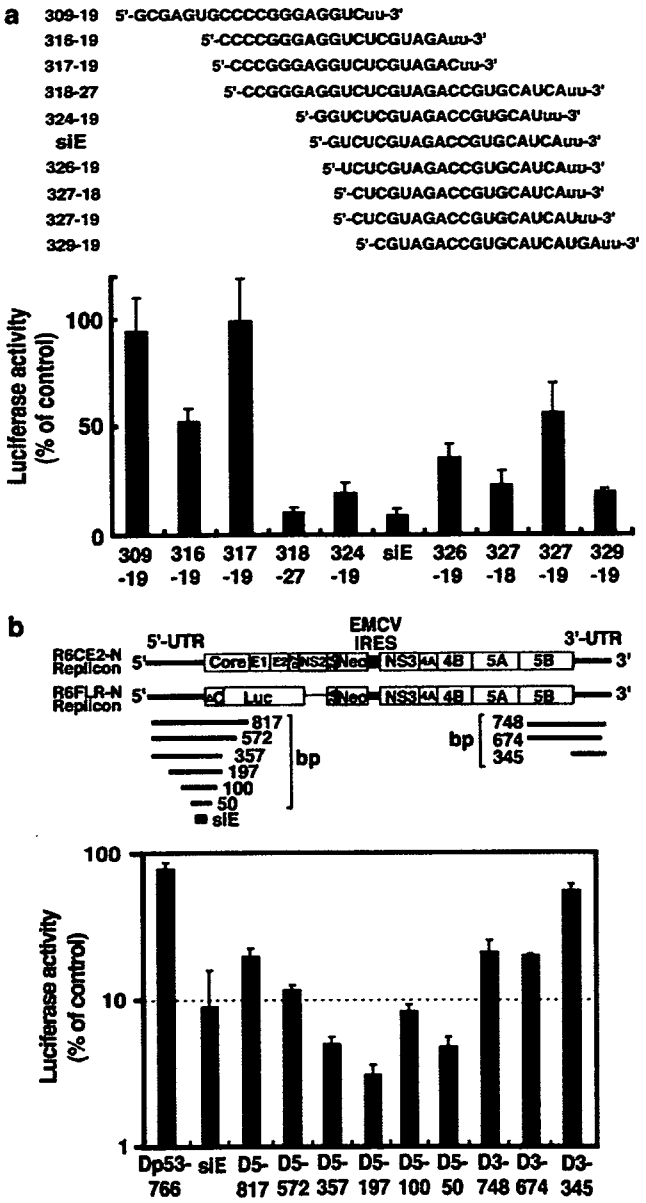

Figure 2 Small interfering RNAs cleaved by rhDicer from long dsRNA. (a) Effect of the positional variations in the siE region. R6FLR-N replicon cells were transfected using Lipofectamine 2000 with siRNAs in which the target position was shifted towards either the 5′- or 3′-end of the siE region. Luciferase activity assay measured 48 h after transfection with 1 nM siRNAs. Data represent means ± s.d. compared with mock-transfected cells ($n = 5$). (b) Upper panel, schematic representation of the long dsRNAs used for targeting different sites in the HCV genome RNA; lower panel, effect of d-siRNAs. The d-siRNAs were generated from the long dsRNAs by cleavage with rhDicer. R6FLR-N cells were transfected with d-siRNAs. Luciferase activity was measured after 48 h. Data represent means ± s.d. compared with mock-transfected cells ($n = 5$). Dp53-766, which targeted p53 mRNA (766 bp), was used as a negative control.

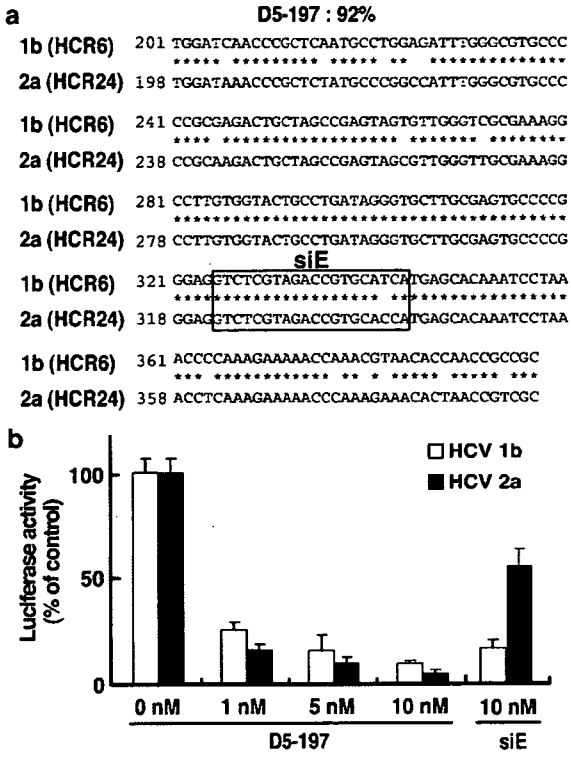

Figure 3 Dicer-generated siRNAs directed at the HCV genotype 2a can cause silencing of genotype 1b RNA. (a) The sequence homology between genotypes 1b and 2a was 92% within the 197-bp region (182/197 nt) and 95% within the 20-bp siE region (19/20 nt). (b) R6FLR-N cells harboring the genotype 1b HCV replicon RNA were transfected with the d-siRNAs generated from a 197-bp dsRNA directed at HCV genotype 2a (HCR24; accession number AY746460). Data represent means ± s.d. compared with mock-transfected cells ($n = 5$).

thetic RNA duplexes 25–30 nt in length are substrates of the dicer endonuclease, directly linking the production of siRNAs to incorporation in the RNA-induced silencing complex. We also expected that intracellular dsRNA duplexes longer than 50 nt would be recognized by dicer and thus induce RNAi. Therefore, we directly transfected long dsRNA into R6CE2-N replicon cells, which harbor the core to NS2 portion of the HCV genome (Figure 2b). The same amount of dsRNA was transfected into replicon cells, and the replicon copy number was determined by quantitative real-time detection (RTD)-polymerase chain reaction (PCR).[24] We found that, except for the 817-bp dsRNA, the long dsRNAs targeting sites in the HCV genome reduced the HCV RNA copy number. In contrast, an unrelated dsRNA targeting a site in endogenous p53 mRNA had no effect (Figure 4a). A luciferase assay in R6FLR-N replicon cells showed similar results for HCV-specific silencing (data not shown). On the other hand, immunoblot analysis with antibodies against p53 showed that p53-specific long dsRNA suppressed the level of p53 protein, whereas HCV-specific dsRNA had no effect on p53 expression (Figure 4b). These results indicated that in HuH-7 replicon cells, direct transfection of long dsRNA can specifically produce RNAi against HCV and reduce endogenous p53 expression.

Effect of long double-stranded RNA on the intracellular interferon response and cell death in HepG2 cells

In mammalian cells, Toll-like receptor (TLR) 3[25,26] recognizes dsRNA duplexes longer than 30 nt. This binding induces a type I IFN response, resulting in cell

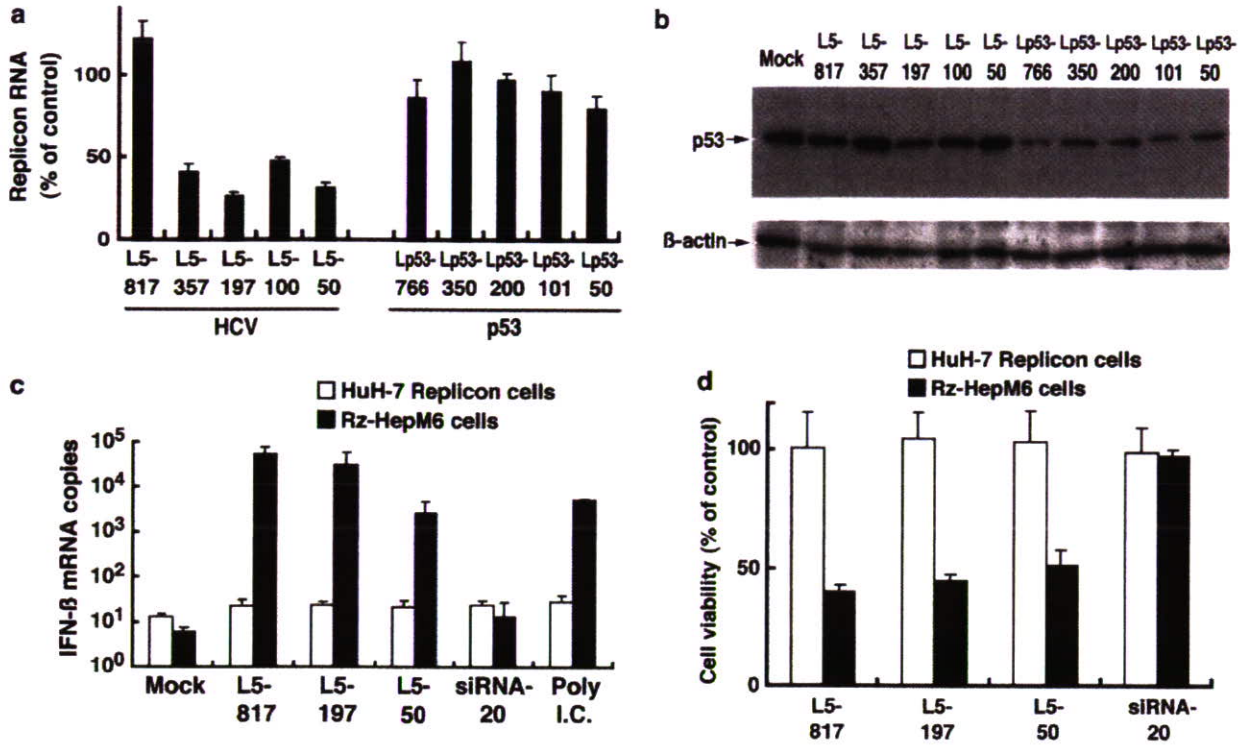

Figure 4 Transfection of long dsRNAs into HuH-7 replicon cells, which lack dsRNA-triggering IFN response, induces target-specific silencing. (**a**) R6CE2-N cells were transfected with long dsRNAs. Replicon RNA levels in cells transfected with 262 ng of dsRNA per 48-well dish were measured after 48 h by RTD–PCR. Data represent means ± s.d. ($n = 3$) of replicon levels compared with mock-transfected cells. (**b**) Immunoblot analysis of p53 and β-actin from replicon cells transfected with dsRNA targeting sites in the HCV genome or p53 mRNA. (**c**) Levels of human IFN-β mRNA were quantified by RTD-PCR 7 h after transfection with 50 ng of dsRNAs per 48-well dish. Values represent the mean copy number for each RNA per μg total RNA ± s.d. ($n = 5$). (**d**) Cell viability was determined after 48 h by WST-8 assay. Data represent means ± s.d. ($n = 3$) of WST conversion compared with mock-transfected cells.

death by apoptosis.[27] To examine the type I IFN response caused by direct transfection of dsRNA, we measured the intracellular IFN-β mRNA copy number and assessed cell viability. The IFN-β mRNA levels of R6FLR-N replicon cells (HuH-7 replicon cells) and the numbers of viable cells did not change following transfection with long dsRNAs or with the RNA duplex poly(rI):poly(rC) (Figures 4c and d). These results show that the dsRNA did not induce intracellular IFN-β mRNA or enhance apoptosis in HuH-7 replicon cells.

HuH-7 replicon cell lines are used as models for HCV replication and do not respond to the IFN signals.[28] We therefore investigated the effect of dsRNAs on the IFN-β response in another cell type. As an alternative model, we used HepG2 cells stably expressing the full genome HCV RNA (Rz-HepM6 cells).[29] Transfection with poly (rI):poly(rC) or long dsRNAs induced an IFN-β mRNA level of 10^3–10^5 copies per μg total RNA, whereas siRNA-20, a 20-nt duplex, induced only 10 copies per μg total RNA (Figure 4c). Furthermore, the number of viable Rz-HepM6 cells was reduced by transfection with long dsRNAs, but not with siRNA-20 (Figure 4d). These results indicated that direct transfection with dsRNA duplex longer than 50 nt induces IFN-β mRNA and causes cytotoxicity in Rz-HepM6 cells, but not in HuH-7 replicon cells. Therefore, to observe the knockdown efficiency of long-dsRNA against the HCV replicating model and the IFN response induced by long dsRNA, we tested the effects of RNAi in HuH-7 replicon, Rz-HepM6 and HepG2 cells.

U6 promoter-driven expression of long hairpin-RNA with mutations in the sense strand causes gene silencing without triggering an interferon response or cell death

We examined the ability of a stable hairpin-type siRNA-expression vector[30–32] to silence the HCV genome. Recently, U6 promoter-driven transcription of hRNA with mutations in the sense strand has been reported to be more effective for RNAi than hRNA containing nonmutated sense strands.[32] Therefore, we constructed vectors for U6 promoter-driven expression of hRNAs containing multiple mutations (mhRNA) and examined their ability to cause gene silencing. To confirm the RNAi effect, we transfected the long mhRNA-expression vectors into R6FLR-N replicon cells. The 50- and 197-bp mhRNA vectors against the HCV sequence reduced luciferase activity as effectively as the siE-20-bp mhRNA vector (Figure 5a). Furthermore, in Rz-HepM6 cells, the 50- and 197-bp mhRNA vectors targeted to the HCV sequence specifically suppressed HCV core protein expression (Figure 5b). To avoid the inhibition of IFN-β activation by HCV itself,[28] we next examined the IFN response in original HepG2 cells. In contrast to the direct transfection of dsRNAs targeted to the same sequences, the 50- and 197-bp mhRNA vectors did not induce the expression of IFN-β mRNA (Figure 5c). Owing to palindrome structure-specific recombination in the mammalian gene,[33] it was not possible to construct stably transformed cells expressing hRNA vectors against the

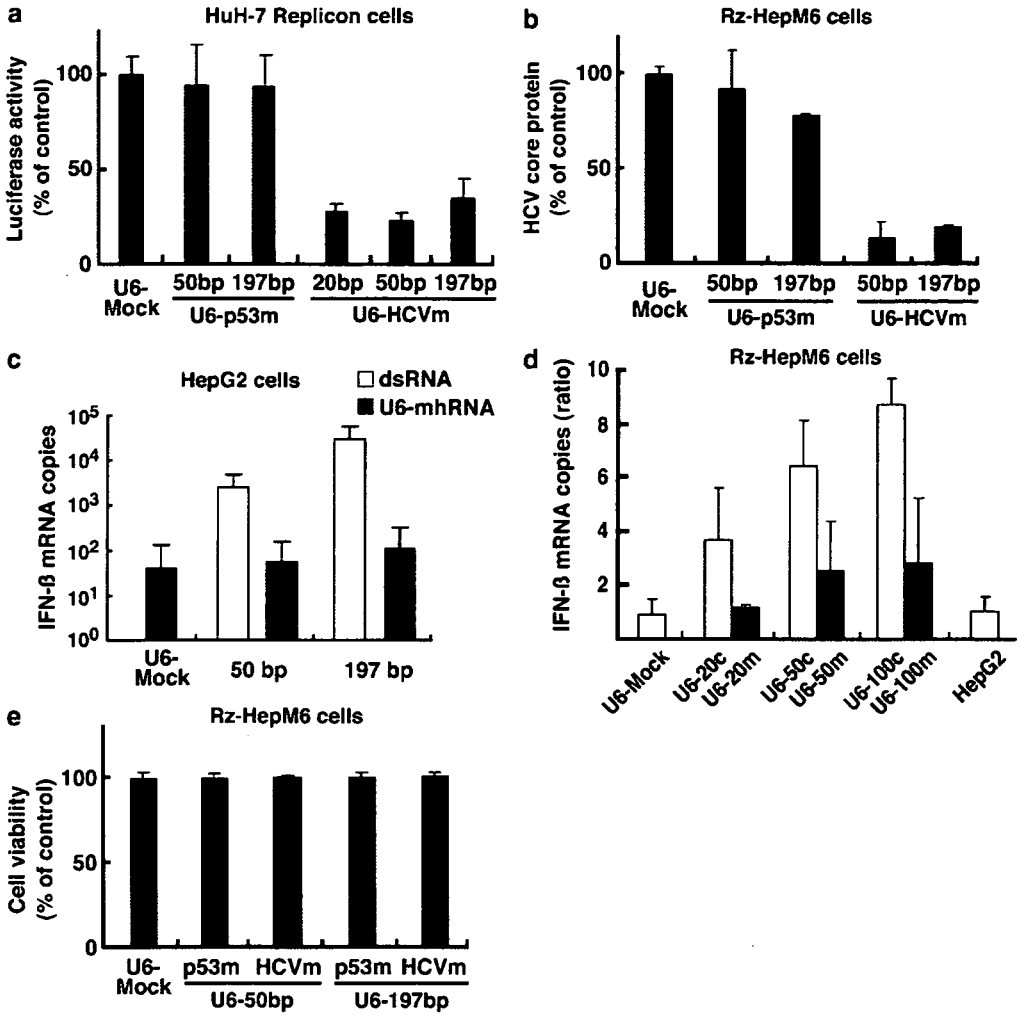

Figure 5 U6 promoter-driven expression of long mhRNA causes gene silencing without triggering an IFN response or cell death. (**a**) U6 promoter-driven transcription of long hRNAs containing multiple point mutations within the sense strand induced RNAi in R6FLR-N replicon cells. Luciferase activity was measured 96 h after transfection with 200 ng vector per 96-well dish. Data represent means ± s.d. compared with control U6 vector-transfected cells ($n = 3$). (**b**) Gene silencing for the long mhRNA-expression vector in Rz-HepM6 cells. All assays were performed 120 h after transfection with 600 ng vector per 48-well dish. Data represent means ± s.d. compared with control U6 vector-transfected cells ($n = 3$). (**c**) Interferon responses in original HepG2 cells following targeting of the same HCV sequences by direct transfection with dsRNA and U6 promoter-driven expression of mhRNA. The level of human IFN-β mRNA was measured by RTD-PCR 7 and 16 h after transfection. Values represent the mean copy numbers for each RNA per μg total RNA ± s.d. ($n = 3$). (**d**) U6 promoter-driven expression of mhRNA caused a lower IFN response in Rz-HepM6 cells than expression of hRNA containing non-mutated sense strands. The level of human IFN-β mRNA was measured by RTD-PCR 16 h after transfection. Values represent the mean ratios compared to control U6 vector-transfected cells ± s.d. ($n = 3$). U6-20c, HCVc-20bp; U6-20m, HCVm-20bp; U6-50c, U6-50m, U6-100c, and U6-100m are U6 vectors against the luciferase gene. (**e**) Cell viability of Rz-HepM6 cells was determined after 120 h by WST-8 assay. Data represent means ± s.d. ($n = 3$) of WST-8 conversion compared with control U6 vector-transfected cells.

HCV sequence containing non-mutated sense strands longer than 50 bp. Using control vectors against the luciferase gene (U6-50c, U6-50m, U6-100c and U6-100m), we confirmed an intracellular IFN response. In Rz-HepM6 cells, all of the mhRNA vectors (HCVm-20 bp, U6-50m and U6-100m) had a reduced IFN response compared to the hRNA vectors containing non-mutated sense strands (HCVc-20 bp, U6-50c and U6-100c; Figure 5d). Moreover, U6 promoter-driven expression of long mhRNAs against the HCV sequence was not cytotoxic (Figure 5e).

These results indicated that in IFN-responsive cells, U6 promoter-driven expression of modified long dsRNA, which be made by inserting multiple mutations in the sense strand of hRNA, can effectively and specifically silence HCV without triggering the IFN response or cell death.

Discussion

Previous studies have shown that HCV RNA can be suppressed by the RNAi machinery in replicon cells.[13–18] We demonstrated that there are two significant limitations for the use of siRNA-mediated RNAi as a therapy for HCV: first, it is difficult to predict which target site will be most effective for siRNA; and, second, it is difficult to target the other HCV genotypes with multiple sequences. We further examined the ability of d-siRNAs and intracellular-diced long dsRNAs to overcome these problems and inhibit HCV replication in HCV replicon

cells. We found that *ex-vivo* dicer-generated siRNAs generated from the 5′-UTR sequences are more effective for silencing than the most potent synthetic siRNA, siE. Our results further demonstrated that 50- and 197-bp dsRNA regions of the HCV genome are potential target areas for RNAi. Although dsRNA duplexes targeting the 50- to 357-bp sites in the HCV genome efficiently cause target silencing, dsRNA duplexes targeting the 817-bp HCV genome are less effective for HCV replication. This suggests that the area of the HCV genome that can be targeted by the RNAi machinery is restricted because of the formation of a complex internal ribosome entry site structure. Recently, Kim *et al.*[23] showed that 27-mer duplexes that are substrates of cellular dicer have enhanced RNAi potency and efficacy in mammalian cells. Our results also suggest that siRNAs generated by dicer from dsRNA duplexes longer than 50 nt are available in their natural form and, therefore, can have enhanced efficacy for RNAi.

In HuH-7 HCV replicon cells, which lack a long dsRNA-induced IFN response, the long dsRNAs were effective at causing RNAi of the HCV genome or endogenous p53. Therefore, we further examined the effect of dsRNA on HepG2 cells, in which dsRNA causes production of IFN-β and activates downstream signaling, including 2′–5′-oligoadenylate synthetase and protein kinase R.[29] Although transfection with dsRNA duplexes longer than 50 nt induced IFN-β and caused cell death, U6 promoter-driven expression of long hRNAs containing multiple point mutations in the sense strand (i.e., near-complementary inverted repeats) efficiently inhibited HCV replication, but was not cytotoxic. Moreover, the intracellular IFN-β mRNA titer was equivalent to that induced by the control U6 vector. The precise mechanism is now under investigation, but it is clear that this system allows intracellular-diced long dsRNA to induce RNAi without activating the IFN response in mammalian cells.

The genotype 2a-derived d-siRNAs generated from the 197-bp dsRNA were able to efficiently inhibit HCV genotype 1b replication. Thus, siRNAs generated from long dsRNA can cause silencing of heterogeneous viruses and should be able to overcome siRNA escape mutations. Long-term HIV-1 replication assays[34] revealed that, after 3–6 weeks of culture, siRNA-mediated RNAi-resistant viruses containing nucleotide substitutions or deletions in the target sequence arise. Wilson *et al.*[35] reported that HCV replicons escaped RNAi induced by subsequent treatment with the same siRNA directed against the NS5B cording region. In contrast, we also examined the long-term efficiency of long dsRNA-mediated RNAi using HCV replicon cells. When examined over 5 weeks with continuous transfection of 197-bp dsRNA, the HCV replicon RNA titer gradually decreased to a 100-fold reduction and never rebounded (data not shown). The degree of sequence conservation reflects the fact that the structural elements in the 5′- and 3′-terminal regions of the RNA are essential for viral replication.[36,37] Therefore, long dsRNA-mediated RNAi targeting a site in the 5′-UTR can avoid the problem of escape virus generation because extensive alterations in a conserved region of the viral genome would be required.

In summary, our results show that dicer-generated siRNAs from long dsRNA are highly effective for RNAi of the HCV genome and overcome genotype variations. We also showed that U6 promoter-driven expression of modified long dsRNA avoids activation of the IFN response and the induction of cell death normally caused by dsRNA. This strategy should be useful for therapy against natural viral infection by HCV and other RNA viruses, such as HIV-1, that display a high rate of mutation.

Materials and methods

Small interfering RNAs

We synthesized T7 siRNAs using the Silencer siRNA Construction Kit (Ambion, Austin, TX, USA) according to the manufacturer's instructions. The sense sequences of siRNAs were as follows:

siA (nt 26–45), 5′-ACUCCACCAUAGAUCACUCCUU-3′;
siB (nt 53–73), 5′-GGAACUACUGUCUUCACGCAGUU-3′;
siC (nt 139–159), 5′-GCCAUAGUGGUCUGCGGAACC UU-3′;
siD (nt 278–299), 5′-AGGCCUUGUGGUACUGCCUGAU UU-3′;
siE (nt 325–344), 5′-GUCUCGUAGACCGUGCAUCAUU-3′;
siF (nt 368–387), 5′-AGAAAAACCAAACGUAACACUU-3′;
siG (nt 9517–9537), 5′-GGCUCCAUCUUAGCCCUAGU CUU-3′;
siH (nt 9540–9560), 5′-GGCUAGCUGUGAAAGGUCCG UUU-3′; and
siI (nt 9553–9572) and 5′-AGGUCCGUGAGCCGCAUGA CUU-3′.

The sense sequence of the p53 m siRNA, which contains two nucleotide mismatches in the target sequence,[38] was 5′-GACUCCAGUGAUAAUCUGCUU-3′ (nucleotide mismatches underlined).

Long double-stranded RNAs

Long dsRNAs were prepared by *in vitro* transcription of PCR-amplified DNA templates. A modified T7 promoter sequence was added to the 5′-end of each PCR primer for amplification (Table 1). The dsRNAs were produced from the purified DNA templates using an Ampliscribe T7 transcription kit (Epicenter Technologies, Madison, WI, USA). Single-stranded RNA was converted to dsRNA by allowing annealing the two strands. Purification of dsRNA was performed as described for dicer-generated siRNAs.

Dicer-generated small interfering RNAs

Digestion with rhDicer (Gene Therapy Systems, San Diego, CA, USA) was carried out according to the manufacturer's protocol. The rhDicer-cleaved siRNAs and dsRNAs were separated by electrophoresis on a nondenaturing 12% polyacrylamide gel and detected by ultraviolet shadowing on a Fluor-coated thin-layer chromatography plate (Ambion). The rhDicer-cleaved siRNAs migrating as 20- to 21-bp bands were excised from the gel and extracted at 37°C for 4 h in extraction buffer (0.5 M ammonium acetate, 1 mM EDTA and 0.2% SDS). Following buffer exchange and desalting by gel filtration with Sephadex G-25 (Amersham Biosciences, Piscataway, NJ, USA), the rhDicer-cleaved siRNAs were dissolved in TE buffer. The cleaved siRNAs were then quantified by adsorption at 260 nm and stored at −70°C.

es, PCR primers and amplicons used for the generation of dsRNAs

	Primer set	*Primer sequence (5' to 3')*	*Amplicon name*	*Start position*	*Stop position*
lb	F-1	GCG TAA TAC GAC TCA CTA TAG GGA GAG AGT GCC CCG GGA GGT CTC GTA GAC	L5-50	311	360
	R-1	GCG TAA TAC GAC TCA CTA TAG GGA GAT TAG GAT TTG TGC TCA TGA TGC ACG			
	F-2	GCG TAA TAC GAC TCA CTA TAG GGA GAT AGT GTT GGG TCG CGA AAG GCC TTG	L5-100	261	360
	R-1	GCG TAA TAC GAC TCA CTA TAG GGA GAT TAG GAT TTG TGC TCA TGA TGC ACG			
	F-3	GCG TAA TAC GAC TCA CTA TAG GGA GAT GGA TCA ACC CGC TCA ATG CCT GGA	L5-197	201	397
	R-2	GCG TAA TAC GAC TCA CTA TAG GGA GAG CGG CGG TTG GTG TTA CGT TTG G			
	F-4	GCG TAA TAC GAC TCA CTA TAG GGA GAA CTC CCC TGT GAG GAA CTA CTG TCT	L5-357	41	397
	R-2	GCG TAA TAC GAC TCA CTA TAG GGA GAG CGG CGG TTG GTG TTA CGT TTG G			
	F-4	GCG TAA TAC GAC TCA CTA TAG GGA GAA CTC CCC TGT GAG GAA CTA CTG TCT	L5-572	41	612
	R-3	GCG TAA TAC GAC TCA CTA TAG GGA GAC CCT CGT TGC CAT AGA GGG GCC A			
	F-4	GCG TAA TAC GAC TCA CTA TAG GGA GAA CTC CCC TGT GAG GAA CTA CTG TCT	L5-817	41	857
	R-4	GCG TAA TAC GAC TCA CTA TAG GGA GAA ACC GGG CAA ATT CCC TGT TGC ATA			
	F-5	GCG TAA TAC GAC TCA CTA TAG GGA GAG CGG GGG AGA GAT ATA TCA CAG C	L3-345	9267	9611
	R-6	GCG TAA TAC GAC TCA CTA TAG GGA GAA CAT GAT CTG CAG AGA GGC CAG T			
	F-6	GCG TAA TAC GAC TCA CTA TAG GGA GAA GGA TGA TTC TGA TGA CCC ATT TCT	L3-674	8864	9537
	R-7	GCG TAA TAC GAC TCA CTA TAG GGA GAG ACT AGG GCT AAG ATG GAG CCA CCA			
	F-6	GCG TAA TAC GAC TCA CTA TAG GGA GAA GGA TGA TTC TGA TGA CCC ATT TCT	L3-748	8864	9611
	R-6	GCG TAA TAC GAC TCA CTA TAG GGA GAA CAT GAT CTG CAG AGA GGC CAG T			
2a	F-2a	GCG TAA TAC GAC TCA CTA TAG GGA GAT GGA TAA ACC CGC TCT ATG CCC GGC	2a-197	198	394
	R-2a	GCG TAA TAC GAC TCA CTA TAG GGA GAG CGA CGG TTA GTG TTT CTT TGG G			
)	F-p1	GCG TAA TAC GAC TCA CTA TAG GGA GAC ATC ACA CTG GAA GAC TCC AG	Lp53-50	1013	1062
	R-p1	GCG TAA TAC GAC TCA CTA TAG GGA GAC AAA GCT GTT CCG TCC CAG TAG			
	F-p2	GCG TAA TAC GAC TCA CTA TAG GGA GAG TGT AAC AGT TCC TGC ATG GG	Lp53-101	962	1062
	R-p1	GCG TAA TAC GAC TCA CTA TAG GGA GAC AAA GCT GTT CCG TCC CAG TAG			
	F-p3	GCG TAA TAC GAC TCA CTA TAG GGA GAG TAT TTG GAT GAC AGA AAC ACT TTT CGA C	Lp53-200	863	1062
	R-p1	GCG TAA TAC GAC TCA CTA TAG GGA GAC AAA GCT GTT CCG TCC CAG TAG			
	F-p4	GCG TAA TAC GAC TCA CTA TAG GGA GAC ACC CGC GTC CGC GCC ATG G	Lp53-350	713	1062
	R-p1	GCG TAA TAC GAC TCA CTA TAG GGA GAC AAA GCT GTT CCG TCC CAG TAG			
	F-p5	GCG TAA TAC GAC TCA CTA TAG GGA GAG CAA TGG ATG ATT TGA TGC TG	Lp53-766	366	1131
	R-p2	GCG TAA TAC GAC TCA CTA TAG GGA GAC CCC TTT CTT GCG GAG ATT C			

stranded RNA; PCR = polymerase chain reaction.
on number.

Construction of U6 vectors

Plasmids containing a human U6 promoter were prepared as described previously.[30] A series of long-hairpin-RNA expression vectors was constructed by inserting a sense sequence between the U6 promoter and the corresponding antisense sequence. Sequences downstream of the U6 promoter were as follows (nucleotide substitutions underlined and loop sequence indicated in lowercase letters):

HCVc-20 bp, 5′-GTCTCGTAGACCGTGCATCAtagaatt acatcaagggagatTGATGCACGGTCTACGAGACTTTTT-3′;

HCVm-20 bp, 5′-GTCTTGTAGATTGTGTATTAtagaatt acatcaagggagatTGATGCACGGTCTACGAGACTTTTT-3′;

p53m-50 bp, 5′-CATTACATTGGAGGATTCCAGTGGT GATCTATTGGGGCGGAGTAGCTTTGgtgtgctgtccCA AAGCTGTTCCGTCCCAGTAGATTACCACTGGAGT CTTCCAGTGTGATGTTTTT-3′;

HCVm-50 bp, 5′-GAGTGTTCTGGGAGGTTTCGTAG ATCGTGTATCGTGAGTACAAGTTCTAAgtgtgctgtccT TAGGATTTGTGCTCATGATGCACGGTCTACGAGA CCTCCCGGGGCACTCTTTTT-3′;

p53m-197 bp, 5′-GTGTTTGGGTGATAGAGACACCTC TCGGCATGGTGTGGTGGTGTCTTATGAGTCGCT TGGGGTTGGTTCTGATTGTATCACTATCTATTACA GCTACGTGTGTGATAGTTCTTGTATGGGTGGCATG GACCGGGGGTCCATTCTCATCATTATCGCACTGG GAGATTCTAGTGGTGATCTATTGGGGCGGGACGG CTTTGgtgtgctgtccCAAAGCTGTTCCGTCCCAGTAG ATTACCACTGGAGTCTTCCAGTGTGATGATGGTG AGGATGGGCCTCCGGTTCATGCCGCCCATGCAG GAACTGTTACACATGTAGTTGTAGTGGATGGTGG TACAGTCAGAGCCAACCTCAGGCGGCTCATAGG GCACCACCACACTATGTCGAGAAGTGTTTCTGTC ATCCAAATACTTTTT-3′;

HCVm-197 bp, 5′-ATGGGTCAGCTCGTTCAATGCTT GGAGGTTTGGGTGTGTCCTCGTGAGATTGCTAGT CGAGTGGTGTTGGGTTGCGGAAGGTCTTGTGGTG CTGTCTGATGGGGTGTTTGTGAGTGTCCTGGGAG GTTTCGTTGACTGTGCATTATGAGTACAGATCCTA GACCTCAGAGAAGGACCAGACGTGACATCAACT GCCGCgtgtgctgtccGCGGCGGTTGGTGTTACGTTTG GTTCTTCTTTGGGGTTTAGGATTTGTGCTCATGAT GCACGGTCTACGAGACCTCCCGGGGCACTCGCA AGCACCCTATCAGGCAGTACCACAAGGCCTTTC GCGACCCAACACTACTCGGCTAGCAGTCTCGCG GGGGCACGCCCAAATCTCCAGGCATTGAGCGGG TTGATCCATTTTT-3′;

U6-50c, 5′-GCCTTCAGGATTACAAGATTCAAAGTG CGCTGCTGGTGCCAACCCTATCTttcaagagaGAATA GGGTTGGCACCAGCAGCGCACTTTGAATCTTGTA ATCCTGAAGGCTTTTT-3′;

U6-50m, 5′- GCCTTTAGGATTATAAGGTTCAAAGTG TGCTGTTGGTGTCAACTCTATCTttcaagagaGAATAG GGTTGGCACCAGCAGCGCACTTTGAATCTTGTAA TCCTGAAGGCTTTTT -3′;

U6-100c, 5′-GATTTCGAGTCGTCTTAATGTATAGATT TGAAGAAGAGCTGTTTCTGAGGAGCCTTCAGGA TTACAAGATTCAAAGTGCGCTGCTGGTGCCAACC CTATTCttcaagagaGAATAGGGTTGGCACCAGCAGC GCACTTTGAATCTTGTAATCCTGAAGGCTCCTCA GAAACAGCTCTTCTTCAAATCTATACATTAAGAC GACTCGAAATCTTTTT-3′ and

U6-100m, 5′-GATTTCGGGTTGTCTTGATGTATGGGT TTGGAGAGGAGTTGTTTCTGGGGAGTCTTTAGGA TTATAAGGTTCAAAGTGTGCTGTTGGTGTCAACT CTATTCttcaagagaGAATAGGGTTGGCACCAGCAGC GCACTTTGAATCTTGTAATCCTGAAGGCTCCTCA GAAACAGCTCTTCTTCAAATCTATACATTAAGAC GACTCGAAATCTTTTT-3′.

Construction of recombinant plasmids for expressing the hepatitis C virus replicon

The HCV genotype 1b replicon pRep-R6FLR-NRz was assembled and cloned from pRep-R6Rz and the 1bneo/delS plasmid.[39] Replicon pRep-R6Rz was engineered from pHCR6-Rz[29] as described previously,[20] and replicon pRep-R6-NRz was engineered by replacing a NS3-NS5B fragment (nt 3420–7996; *Mfe*I site) in pRep-R6Rz with a NS3-NS5B fragment (nt 3420–7996; *Mfe*I site) from the 1bneo/delS plasmid. The final replicon, pRep-R6FLR-NRz, was constructed by replacing the neomycin phosphotransferase (*neo*^{r}) gene of pRep-R6-NRz with a chimeric gene encoding firefly luciferase protein fused in-frame with the 2A genes of FMDV and *neo*^{r}.

The HCV genotype 1b replicon pRep-R6CE2-NRz was assembled and cloned from pRep-R6-NRz and pHCR6-Rz. Plasmid pRep-R6CE2-NRz was engineered by replacing the HCV internal ribosome entry site gene (nt 1–389) in pRep-R6-NRz with a Core-NS2 gene (nt 1–3030; *Rsr*II site) from the pHCR6 plasmid. The pRep-R6CE2-NRz replicon was constructed by fusing the HCV NS2 protein gene in-frame with the genes for FMDV 2A protein and *neo*^{r}.

Cell culture and transfection

We maintained the human hepatoma cell line HuH-7 in complete Dulbecco's modified Eagle medium (DMEM; Invitrogen, Carlsbad, CA, USA). G418 was added to a final concentration of 500 μg/ml to cell lines carrying HCV replicons.[20] Replicon cells were transfected with synthetic siRNA using Trans IT TKO reagent (Mirus, Madison, WI, USA) or with modified siE, dicer-generated siRNAs, long dsRNA and DNA vector using Lipofectamine 2000 (Invitrogen) according to the manufacturer's protocol. Also, Rz-HepM6 cells[29] were transfected with various amounts of dsRNAs or DNA vector using Lipofectamine 2000.

Luciferase assays

The luciferase assay was performed using the Steady-Glo or Bright-Glo luciferase assay systems (Promega). Luciferase activities were quantified using a luminometer (Mithras LB940; Berthold Technologies, Wildbad, Germany).

Cell viability assay

To evaluate the cytotoxic effects of dsRNAs, cell viability was measured by metabolic conversion of 2-(2-methoxy-4-nitrophenyl)-3-(4-nitrophenyl)-5-(2,4-disulfophenyl)-2H-tetrazolium, monosodium salt (WST-8) using a Cell Counting Kit-8 (Wako, Tokyo, Japan) according to the manufacturer's protocol.

Immunoblot analysis

Immunoblot analysis was performed as described previously.[29] Anti-p53 (Novocastra Laboratories Ltd, Newcastle Upon Tyne, UK) and anti-β-actin (Santa Cruz Biotechnology, Santa Cruz, CA, USA) were used as the primary antibodies.

Real-time detection–polymerase chain reaction analysis

The HCV genome RNA and IFN-β mRNA were quantified using the ABI PRISM 7700 sequence detector (Applied Biosystems, Foster City, CA, USA) as described previously.[24,29]

Quantification of hepatitis C virus core protein

Hepatitis C virus core protein was assessed in cell lysates using a fluorescent enzyme-linked immunosorbent assay.[40]

Acknowledgements

We express their gratitude to Dr Christoph Seeger (Institute for Cancer Research, Fox Chase Cancer Center, Philadelphia, PA) for his kind gift of the replicon plasmid. We also thank Ms Etsuko Endo for creating the figures. This study was supported by grants from the Ministry of Education, Culture, Sports, Science and Technology of Japan; the Program for Promotion of Fundamental Studies in Health Sciences of the National Institute of Biomedical Innovation of Japan, and the Ministry of Health, Labor and Welfare of Japan.

References

1 WHO. Hepatitis C – global prevalence (update). *Wkly Epidemiol Rec* 2000; **75**: 18–19.
2 Chander G, Sulkowski MS, Jenckes MW, Torbenson MS, Herlong HF, Bass EB *et al.* Treatment of chronic hepatitis C: a systematic review. *Hepatology* 2002; **36**: S135–S144.
3 Tsukiyama-Kohara K, Iizuka N, Kohara M, Nomoto A. Internal ribosome entry site within hepatitis C virus RNA. *J Virol* 1992; **66**: 1476–1483.
4 Tanaka T, Kato N, Cho MJ, Shimotohno K. A novel sequence found at the 3′ terminus of hepatitis C virus genome. *Biochem Biophys Res Commun* 1995; **215**: 744–749.
5 Bukh J, Miller RH, Purcell RH. Genetic heterogeneity of hepatitis C virus: quasispecies and genotypes. *Semin Liver Dis* 1995; **15**: 41–63.
6 Martell M, Esteban JI, Quer J, Genesca J, Weiner A, Esteban R *et al.* Hepatitis C virus (HCV) circulates as a population of different but closely related genomes: quasispecies nature of HCV genome distribution. *J Virol* 1992; **66**: 3225–3229.
7 Behrens SE, Tomei L, De Francesco R. Identification and properties of the RNA-dependent RNA polymerase of hepatitis C virus. *EMBO J* 1996; **15**: 12–22.
8 Sullenger BA, Gilboa E. Emerging clinical applications of RNA. *Nature* 2002; **418**: 252–258.
9 Hannon GJ. RNA interference. *Nature* 2002; **418**: 244–251.
10 Elbashir SM, Harborth J, Lendeckel W, Yalcin A, Weber K, Tuschl T. Duplexes of 21-nucleotide RNAs mediate RNA interference in cultured mammalian cells. *Nature* 2001; **411**: 494–498.
11 Jacque JM, Triques K, Stevenson M. Modulation of HIV-1 replication by RNA interference. *Nature* 2002; **418**: 435–438.
12 Gitlin L, Karelsky S, Andino R. Short interfering RNA confers intracellular antiviral immunity in human cells. *Nature* 2002; **418**: 430–434.
13 Randall G, Grakoui A, Rice CM. Clearance of replicating hepatitis C virus replicon RNAs in cell culture by small interfering RNAs. *Proc Natl Acad Sci USA* 2003; **100**: 235–240.
14 Kronke J, Kittler R, Buchholz F, Windisch MP, Pietschmann T, Bartenschlager R *et al.* Alternative approaches for efficient inhibition of hepatitis C virus RNA replication by small interfering RNAs. *J Virol* 2004; **78**: 3436–3446.
15 Kapadia SB, Brideau-Andersen A, Chisari FV. Interference of hepatitis C virus RNA replication by short interfering RNAs. *Proc Natl Acad Sci USA* 2003; **100**: 2014–2018.
16 Wilson JA, Jayasena S, Khvorova A, Sabatinos S, Rodrigue-Gervais IG, Arya S *et al.* RNA interference blocks gene expression and RNA synthesis from hepatitis C replicons propagated in human liver cells. *Proc Natl Acad Sci USA* 2003; **100**: 2783–2788.
17 Seo MY, Abrignani S, Houghton M, Han JH. Small interfering RNA-mediated inhibition of hepatitis C virus replication in the human hepatoma cell line Huh-7. *J Virol* 2003; **77**: 810–812.
18 Yokota T, Sakamoto N, Enomoto N, Tanabe Y, Miyagishi M, Maekawa S *et al.* Inhibition of intracellular hepatitis C virus replication by synthetic and vector-derived small interfering RNAs. *EMBO Rep* 2003; **4**: 602–608.
19 Okamoto H, Kurai K, Okada S, Yamamoto K, Lizuka H, Tanaka T *et al.* Full-length sequence of a hepatitis C virus genome having poor homology to reported isolates: comparative study of four distinct genotypes. *Virology* 1992; **188**: 331–341.
20 Lohmann V, Korner F, Koch J, Herian U, Theilmann L, Bartenschlager R. Replication of subgenomic hepatitis C virus RNAs in a hepatoma cell line. *Science* 1999; **285**: 110–113.
21 Kawasaki H, Suyama E, Iyo M, Taira K. siRNAs generated by recombinant human Dicer induce specific and significant but target site-independent gene silencing in human cells. *Nucleic Acids Res* 2003; **31**: 981–987.
22 Bernstein E, Caudy AA, Hammond SM, Hannon GJ. Role for a bidentate ribonuclease in the initiation step of RNA interference. *Nature* 2001; **409**: 363–366.
23 Kim DH, Behlke MA, Rose SD, Chang MS, Choi S, Rossi JJ. Synthetic dsRNA Dicer substrates enhance RNAi potency and efficacy. *Nat Biotechnol* 2005; **23**: 222–226.
24 Takeuchi T, Katsume A, Tanaka T, Abe A, Inoue K, Tsukiyama-Kohara K *et al.* Real-time detection system for quantification of hepatitis C virus genome. *Gastroenterology* 1999; **116**: 636–642.
25 Matsumoto M, Kikkawa S, Kohase M, Miyake K, Seya T. Establishment of a monoclonal antibody against human Toll-like receptor 3 that blocks double-stranded RNA-mediated signaling. *Biochem Biophys Res Commun* 2002; **293**: 1364–1369.
26 Oshiumi H, Matsumoto M, Funami K, Akazawa T, Seya T. TICAM-1, an adaptor molecule that participates in Toll-like receptor 3-mediated interferon-beta induction. *Nat Immunol* 2003; **4**: 161–167.
27 Takaoka A, Hayakawa S, Yanai H, Stoiber D, Negishi H, Kikuchi H *et al.* Integration of interferon-alpha/beta signalling to p53 responses in tumour suppression and antiviral defence. *Nature* 2003; **424**: 516–523.
28 Foy E, Li K, Wang C, Sumpter Jr R, Ikeda M, Lemon SM *et al.* Regulation of interferon regulatory factor-3 by the hepatitis C virus serine protease. *Science* 2003; **300**: 1145–1148.
29 Tsukiyama-Kohara K, Tone S, Maruyama I, Inoue K, Katsume A, Nuriya H *et al.* Activation of the CKI–CDK–Rb–E2F pathway in full genome hepatitis C virus-expressing cells. *J Biol Chem* 2004; **279**: 14531–14541.
30 Miyagishi M, Taira K. U6 promoter-driven siRNAs with four uridine 3′ overhangs efficiently suppress targeted gene expression in mammalian cells. *Nat Biotechnol* 2002; **20**: 497–500.
31 Miyagishi M, Taira K. Strategies for generation of an siRNA expression library directed against the human genome. *Oligonucleotides* 2003; **13**: 325–333.

32 Miyagishi M, Sumimoto H, Miyoshi H, Kawakami Y, Taira K. Optimization of an siRNA-expression system with an improved hairpin and its significant suppressive effects in mammalian cells. *J Gene Med* 2004; **6**: 715–723.
33 Tanaka H, Tapscott SJ, Trask BJ, Yao MC. Short inverted repeats initiate gene amplification through the formation of a large DNA palindrome in mammalian cells. *Proc Natl Acad Sci USA* 2002; **99**: 8772–8777.
34 Das AT, Brummelkamp TR, Westerhout EM, Vink M, Madiredjo M, Bernards R *et al*. Human immunodeficiency virus type 1 escapes from RNA interference-mediated inhibition. *J Virol* 2004; **78**: 2601–2605.
35 Wilson JA, Richardson CD. Hepatitis C virus replicons escape RNA interference induced by a short interfering RNA directed against the NS5b coding region. *J Virol* 2005; **79**: 7050–7058.
36 Yanagi M, St Claire M, Emerson SU, Purcell RH, Bukh J. *In vivo* analysis of the 3′ untranslated region of the hepatitis C virus after *in vitro* mutagenesis of an infectious cDNA clone. *Proc Natl Acad Sci USA* 1999; **96**: 2291–2295.
37 Bartenschlager R, Lohmann V. Replication of hepatitis C virus. *J Gen Virol* 2000; **81**: 1631–1648.
38 Brummelkamp TR, Bernards R, Agami R. A system for stable expression of short interfering RNAs in mammalian cells. *Science* 2002; **296**: 550–553.
39 Guo JT, Bichko VV, Seeger C. Effect of alpha interferon on the hepatitis C virus replicon. *J Virol* 2001; **75**: 8516–8523.
40 Tanaka T, Lau JY, Mizokami M, Orito E, Tanaka E, Kiyosawa K *et al*. Simple fluorescent enzyme immunoassay for detection and quantification of hepatitis C viremia. *J Hepatol* 1995; **23**: 742–745.

THE JOURNAL OF IMMUNOLOGY

CUTTING EDGE

Cutting Edge: Lentiviral Short Hairpin RNA Silencing of PTEN in Human Mast Cells Reveals Constitutive Signals That Promote Cytokine Secretion and Cell Survival[1]

Yasuko Furumoto, Steve Brooks,* Ana Olivera,* Yasuomi Takagi,‖ Makoto Miyagishi,¶ Kazunari Taira,¶ Rafael Casellas,† Michael A. Beaven,§ Alasdair M. Gilfillan,‡ and Juan Rivera[2]**

Engagement of the FcεRI expressed on mast cells induces the production of phosphatidylinositol 3, 4, 5-trisphosphate by PI3K, which is essential for the functions of the cells. PTEN (phosphatase and tensin homologue deleted on chromosome ten) directly opposes PI3K by dephosphorylating phosphatidylinositol 3, 4, 5-trisphosphate at the 3′ position. In this work we used a lentivirus-mediated short hairpin RNA gene knockdown method to study the role of PTEN in CD34$^+$ peripheral blood-derived human mast cells. Loss of PTEN caused constitutive phosphorylation of Akt, p38 MAPK, and JNK, as well as cytokine production and enhancement in cell survival, but not degranulation. FcεRI engagement of PTEN-deficient cells augmented signaling downstream of Src kinases and increased calcium flux, degranulation, and further enhanced cytokine production. PTEN-deficient cells, but not control cells, were resistant to inhibition of cytokine production by wortmannin, a PI3K inhibitor. The findings demonstrate that PTEN functions as a key regulator of mast cell homeostasis and FcεRI- responsiveness. The Journal of Immunology, 2006, 176: 5167–5171.

There is increasing evidence that key steps in mast cell activation are mediated through the enzymatic activity of PI3K (1–4), whose product, phosphatidylinositol 3,4,5-trisphosphate (PIP_3),[3] binds to the pleckstrin homology domain of various signaling proteins, allowing their activation and targeting to the membrane and cytoskeleton. Because of the diversity of signaling proteins regulated by PIP_3, this lipid has broad effects on cell signaling and function. For example, mutation of the p110δ catalytic subunit of PI3K (4) and the genetic deletion of the Fyn kinase or of the adapter Gab2 (both of which regulate PI3K activity) (2, 3) significantly impaired FcεRI-mediated mast cell responses. In contrast, genetic loss of Lyn kinase or SHIP-1 (a 5′-phosphatase of PIP_3) increased intracellular PIP_3 levels (3, 5) and augmented FcεRI-mediated mast cell responses (5, 6). Thus, understanding how PIP_3 levels are regulated and what responses might be most sensitive to this lipid should provide new insights on its importance in cellular function.

PTEN (phosphatase and tensin homologue deleted on chromosome ten) opposes PI3K function by dephosphorylating the 3′ position of PIP_3. PTEN is a known tumor suppressor and a key regulator of cell growth and apoptosis (7). Although PTEN knockout mice are embryonic lethal, $PTEN^{+/-}$ mice develop an autoimmune disorder characterized by increased numbers of activated T cells and polyclonal lymphoid hyperplasia (8), demonstrating its importance in immune cell regulation.

To address the question of whether the aforementioned increase in PIP_3 was key in the hyperresponsiveness phenotype of Lyn- and SHIP-null mast cells (3, 5), we down-regulated PTEN expression in mast cells. Human mast cells provided the most suitable model for our studies due to their slow proliferation and nondetectable levels of PI3K activity in resting conditions (9). However, the genetic manipulation of these cells has been difficult to achieve. We speculated that the HIV-related lentivirus might prove useful in gene manipulation of these cells. We coupled this vector technology with the introduction of short hairpin RNA (shRNA) for sequence-specific posttranscriptional gene silencing. Using this approach, we now find that PTEN is a key regulator of mast cell homeostasis and function.

Materials and Methods

Antibodies and reagents

All Abs and reagents used in this study have been described elsewhere (3, 6, 9, 10). Biotinylated human IgE was obtained as described (9). Streptavidin (SA) was from Sigma-Aldrich. Secondary Abs were previously described (10).

*Molecular Inflammation Section and †Genomic Integrity Group, Molecular Immunology and Inflammation Branch, National Institute of Arthritis and Musculoskeletal and Skin Diseases, ‡Laboratory of Allergic Diseases, National Institute of Allergy and Infectious Diseases, and §Laboratory of Molecular Immunology, National Heart, Lung and Blood Institute, National Institutes of Health, Bethesda, MD 20892; ¶Department of Chemistry and Biotechnology, School of Engineering, University of Tokyo, Tokyo, Japan; and ‖iGENE Therapeutics Inc., Tsukuba Science City, Japan

Received for publication January 24, 2006. Accepted for publication March 6, 2006.

The costs of publication of this article were defrayed in part by the payment of page charges. This article must therefore be hereby marked *advertisement* in accordance with 18 U.S.C. Section 1734 solely to indicate this fact.

[1] This research was supported in part by the Intramural Research Program of the National Institutes of Health.

[2] Address correspondence and reprint requests to Dr. Juan Rivera, National Institute of Arthritis and Musculoskeletal and Skin Diseases /National Institutes of Health, Building 10, Room 9N228, Bethesda, MD 20892-1820. E-mail address: juan_rivera@nih.gov

[3] Abbreviations used in this paper: PIP_3, phosphatidylinositol 3,4,5-trispohosphate; ATF2, activating transcription factor 2; HMC-1, human mast cell line 1; HuMC, human mast cell; IKK, IκB kinase; LAT, linker for activation of T cells; PLCγ, phospholipase Cγ; PTEN, phosphatase and tensin homologue deleted on chromosome ten; SA, streptavidin; shRNA, short hairpin RNA.

0022-1767/06/$02.00

Lentivirus shRNA vector construction and gene transduction

The entry vector (pEnter/U6) containing a U6 promoter, a double strand oligonucleotide, and a polymerase III terminator was used to transfer the U6 RNAi cassette into the lentiviral expression plasmid (pLenti6/BLOCK-iT-DEST) using Gateway Technology (Invitrogen Life Technologies). Recombination was performed with the pENTR/U6 entry construct and pLenti6/BLOCK-iT-DEST to generate the pLenti6/BLOCK-iT. The sense and antisense oligonucleotide sequence for construction of four PTEN (GenBank accession number NM_000314) shRNAs were as follows: PTEN no. 1 sense, 5′-CAC CGG GAT AAT ATT GAT GGT GTA CGT GTG CTG TCC GTA CAT CAT CAA TAT TGT TCC-3′, and PTEN no. 1 antisense, 5′-AAA AGG AAC AAT ATT GAT GAT GTA CGG ACA GCA CAC GTA CAC CAT CAA TAT TAT CCC-3′; PTEN no. 2 sense, 5′-CAC CGA GTG GGT TTG AAA TAT TAA CGT GTG CTG TCC GTT AAT GTT TCA AGC CCA TTC-3′, and PTEN no. 2 antisense, 5′-AAA AGA ATG GGC TTG AAA CAT TAA CGG ACA GCA CAC GTT AAT ATT TCA AAC CCA CTC-3′; PTEN no. 3 sense, 5′-CAC CGA TTT AGG CTT GAC TTA TAA CGT GTG CTG TCC GTT ATA GGT CAA GTC TAA GTC-3′, and PTEN no. 3 antisense, 5′-AAA AGA CTT AGA CTT GAC CTA TAA CGG ACA GCA CAC GTT ATA AGT CAA GCC TAA ATC-3′; and PTEN no. 4 sense, 5′-CAC CGG GCT AGA GGA AAC TTC ATA CGT GTG CTG TCC GTA TGA GGT TTC CTC TGG TCC-3′, and antisense, 5′-AAA AGG ACC AGA GGA AAC CTC ATA CGG ACA GCA CAC GTA TGA AGT TTC CTC TAG CCC-3′.

Packaging vector (9 μg) (ViraPower packaging mix; Invitrogen Life Technologies), pLenti6/Block-iT with PTEN shRNA or control LacZ shRNA, or GFP expressing pNUTS vector (6 μg), were cotransfected into 293FT packaging cells with Lipofectamine 2000 (35 μl) (Invitrogen Life Technologies). After 48 h the culture supernatants were centrifuged to pellet the released virus and resuspended in 5 ml of StemPro medium. Transduction of human mast cells (HuMCs) or human mast cell line 1 (HMC-1) cells (5×10^6) was conducted by resuspending the cells in the 5 ml of virus containing StemPro medium. Two days after infection, the medium was changed to virus-free Stem Pro, and antibiotic selection (2 μg/ml blasticidin) was initiated following an additional 2-day recovery. After 3 wk of selection, cells were analyzed for FcεRI expression. Cultures were used when >95% of the cells expressed FcεRI.

Cell cultures, activation, lysates, and immunoblots.

The HMC-1 mast cell line was cultured as described (11). HuMCs were developed from $CD34^+$ cells as described (9). Experiments were conducted 8–10 wk after the initiation of HuMC cultures (99% mast cells). FcεRI stimulation of HuMCs (sensitized with biotinylated IgE) was accomplished with the indicated concentration of SA. Lysates were prepared and proteins identified as described (12).

Measurement of cytosolic calcium, degranulation, cytokine production, PIP_3, and apoptosis

Calcium measurements on fura-2 loaded HuMCs were previously described (13). Release (degranulation) of the granule marker β-hexosaminidase was assayed as previously described (9). For cytokine secretion, the human cytokine array ELISA kit from Novagen was used (13). PIP_3 isolation and measurements were done as described (3). For initiation of apoptosis, cells were in StemPro medium without IL-6 and stem cell factor for up to 48 h. Detection of changes in mitochondrial membrane potential and DNA compaction was by flow cytometric measurement with tetramethyl rhodamine methyl ester and DNA compaction with ToPro-3, respectively.

Results and Discussion

Lentiviral-mediated expression of genes (GFP) in HMC-1 cells or $CD34^+$-derived cultured HuMCs was highly successful (Fig. 1). The efficiency of the transduction ranged from 70 to 99% for transient expression of GFP in HMC-1 (Fig. 1*B*) or HuMC (Fig. 1*C*). Selection with blasticidin led to stable protein expression or protein down-regulation (with shRNA) for up to 6 wk (Figs. 1 and 2, and data not shown). Four shRNA sequences were chosen for PTEN down-regulation based on a previously described algorithm (14). All four sequences inhibited PTEN protein expression in HMC-1 cells (Fig. 2*A*). The PI3K-dependent kinase 1 (PDK1)-dependent phosphorylation of Akt (T308) was used as a surrogate measure of increased PIP_3 production following PTEN down-regulation (PDK1 is a PIP_3-binding protein). Constitutive phosphorylation of Akt

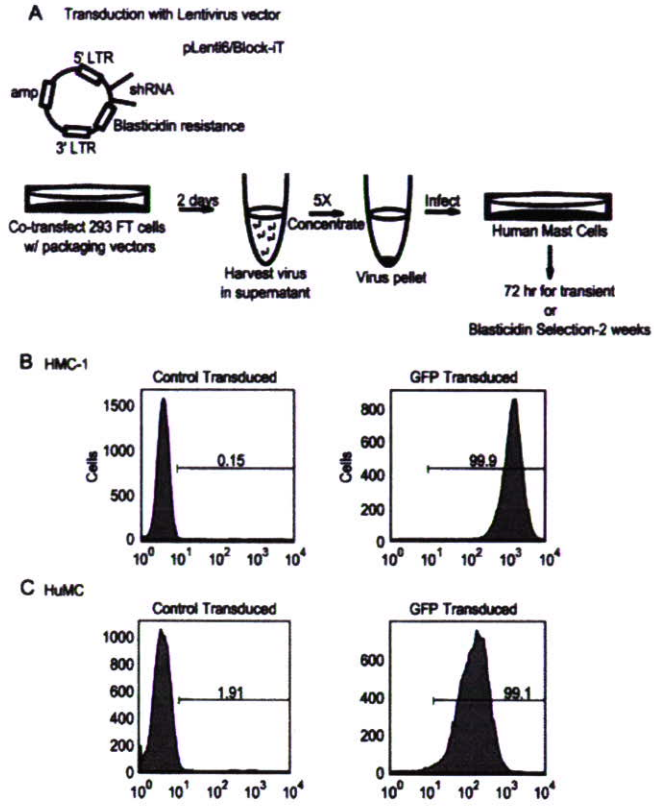

FIGURE 1. Lentivirus-mediated transduction of HuMCs is highly efficient. *A*, Packaging vectors (9 μg) (ViraPower packaging mix; Invitrogen Life Technologies) and pLenti6/Block-iT/PTEN or lacZ shRNA (6 μg) were transfected to 293FT cells. Alternatively, the pNUTS vector carrying a GFP expression cassette was used to assess transduction efficiency. The virus produced was concentrated 5-fold and used to infect 21-day-old cultures of HuMCs. LTR, long terminal repeat; amp, ampicillin-resistance gene. *B* and *C*, Histograms show transient expression of GFP (pNUTS vector) in HMC-1 and HuMCs 4 days after infection. One experiment representative of >10 is shown.

(T308) was increased 3- to 7-fold relative to nontransduced or control lentiviral LacZ shRNA-transduced HMC-1 cells. Direct assessment of PIP_3 production, as shown in Fig. 2*B*, revealed a constitutive increase on the average of 1.5- to 2-fold. Because transduction with shRNA no. 1 resulted in effective loss of PTEN protein (Fig. 2*A*) and in a constitutive increase of at least 2-fold in PIP_3 levels (Fig. 2*B*), this shRNA sequence was used to analyze the role of PTEN in HuMC.

PTEN-deficiency also caused a constitutive phosphorylation of Akt (T308) in HuMCs (Fig. 3*A*). No significant increase in PIP_3 or Akt phosphorylation was observed in control wild-type cells (Figs. 2 and 3), arguing that control of these responses depends on the constitutive activity of PTEN. This differs from SHIP-null murine bone marrow-derived mast cells, where resting cells showed minimal phosphorylation of Akt (5).

After FcεRI-stimulation, Akt (T308) phosphorylation in PTEN-deficient cells was further increased. Akt is well known to function as a PI3K-dependent prosurvival protein through its regulation of Bcl family members, the Forkhead family of transcription factors, and p53 family members (15). Analysis of events that can initiate apoptosis (mitochondrial membrane potential and DNA compaction) under conditions of growth factor starvation revealed a significant reduction (16 h) in these events in PTEN-deficient cells (Fig. 3*B*). Thymidine incorporation studies showed a slight increase (1.5-fold) in the rate of

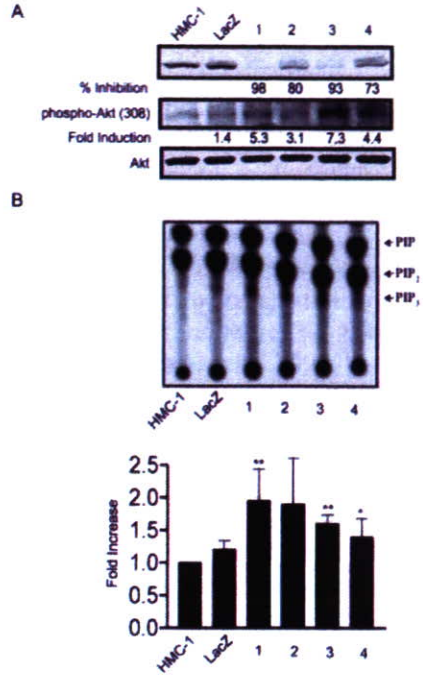

FIGURE 2. Lentiviral shRNA silencing of PTEN increases PIP_3 production and Akt phosphorylation. *A*, Nontransduced HMC-1 cells or cells transduced with LacZ shRNA or four lentiviral shRNA constructs (1–4) were assessed for loss of PTEN and for Akt (T308) phosphorylation (phospho-Akt). PTEN loss is shown as the percentage (%) of inhibition, and fold induction of Akt (T308) phosphorylation is also indicated. *B*, PIP_3 production is enhanced by PTEN down-regulation with four lentiviral shRNA constructs (1–4). Quantitation of all experiments is shown in the h (*, $p < 0.05$; **, $p < 0.01$).

proliferation of PTEN-deficient cells (data not shown). Prolonged growth factor starvation (>48 h), however, caused the death of all cells.

The effect of PTEN-deficiency on FcεRI-initiated signaling was explored. The phosphorylation of Src family kinases in the

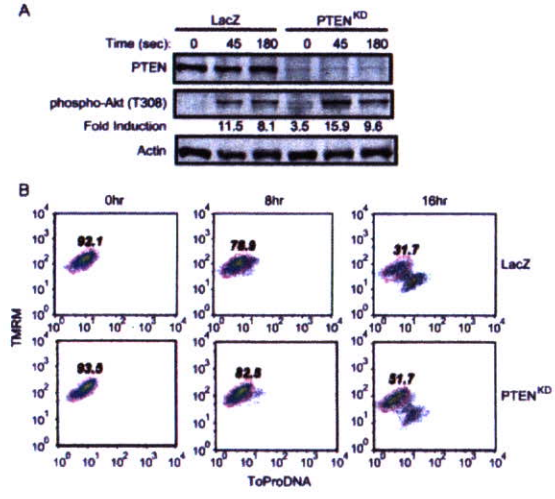

FIGURE 3. PTEN-deficient HuMCs have increased Akt phosphorylation and decreased signals for initiation of apoptosis. *A*, Akt is constitutively phosphorylated (phospho-Akt) in PTEN-deficient HuMCs, and FcεRI stimulation further enhances this event. *B*, IL-6 and the stem cell factor were withdrawn from human mast cell cultures for the indicated times. Initiation of apoptosis was determined using the mitochondrial dye tetramethyl rhodamine methyl ester (TMRM) and the DNA stain ToPro-3 (ToProDNA). The percentage of live/nonapoptotic cells is indicated (red gate). One representative experiment of four is shown.

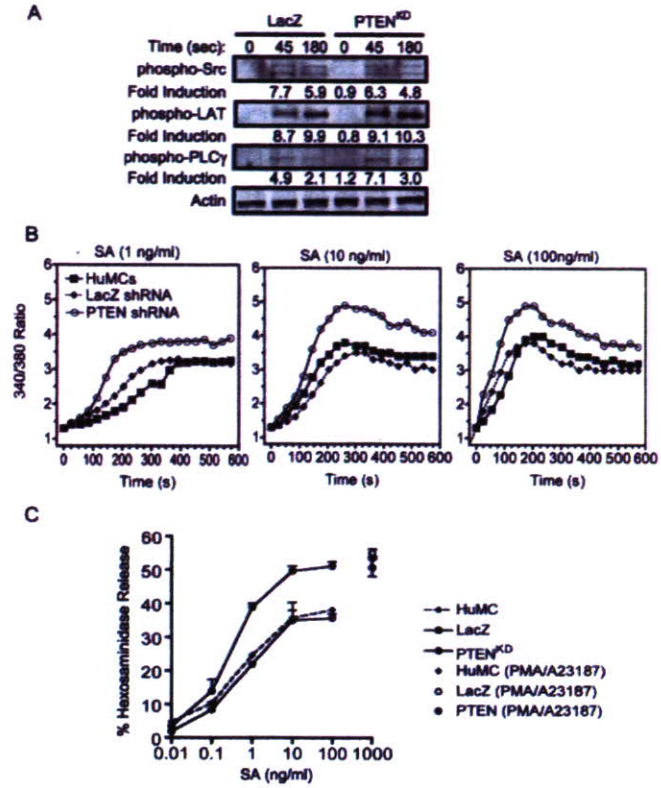

FIGURE 4. PTEN-deficient HuMCs showed increased phosphorylation of PLCγ, calcium mobilization, and degranulation. *A*, Biotinylated IgE-sensitized HuMCs were stimulated or not stimulated with 100 ng/ml SA. The phosphorylation (phospho-) of PLCγ (Y783), LAT (Y191), and Src (Y416) was determined. Actin was used for normalization of protein loading. One representative experiments of three is shown. *B*, fura-2 loaded HuMCs (sensitized as in *A*) were stimulated as indicated to measure intracellular-free Ca^{2+}. The ratio of fluorescence emission at 510 nm when cells are excited at 340 and 380 nm is shown. Data are representative of three experiments using duplicate samples from individual HuMC cultures. The calcium response of HuMC or LacZ controls was not significantly different. *C*, Degranulation from indicated cells was measured by β-hexosaminidase release of IgE-sensitized cells stimulated with 0.01–100 ng/ml SA for 30 min. Maximal degranulation was determined by PMA (20 nM) and the calcium ionophore A23187 (200 nM) stimulation. Degranulation is expressed as the percentage of total intracellular β-hexosaminidase released to the medium. Data are means ± SEM from six individual experiments.

activation loop tyrosine (Y416) was not detected in resting cells but was identically stimulated in control or PTEN-deficient HuMCs (Fig. 4*A*). LAT (linker for activation of T cells) phosphorylation at Y191 contributed to the stability of this signaling complex (16), required FcεRI stimulation, and was independent of PTEN expression. Phosphorylation of phospholipase Cγ, which binds to LAT and hydrolyzes PIP_2, generating inositol 1,4,5-trisphosphate to cause calcium mobilization, was significantly increased (~1.5-fold at 45 s; $p \leq 0.05$) in PTEN-deficient cells (Fig. 4*A*). This was linked to enhanced FcεRI-dependent calcium mobilization in PTEN-deficient HuMCs (Fig. 4*B*) and increased degranulation as compared with control cells (Fig. 4*C*). No differences were observed in basal (spontaneous) degranulation. The results demonstrate that the loss of PTEN is insufficient to initiate a constitutive degranulation response, but the increased phospholipase Cγ (PLCγ) activation and calcium responses seemingly served to enhance FcεRI-stimulated secretion.

The importance of PI3K activity for the de novo synthesis of cytokines in mast cells has been well demonstrated (2, 4); however, the signals influenced by PIP_3 are unclear. MAP kinases (ERK, JNK, and p38) phosphorylate transcription factors known to regulate cytokine gene expression (17). Fig. 5*A* shows that PTEN deficiency caused a minimal constitutive phosphorylation of ERK, whereas constitutive phosphorylation of JNK and p38 reached 60–70% of the stimulated response. Because MAP kinases are linked to transcription factor activation, we analyzed the phosphorylation of IκB kinase (IKK), activating transcription factor 2 (ATF2), and c-Jun. IKK and c-Jun phosphorylation was not significantly altered in PTEN-deficient cells (Fig. 5*B*); however, constitutive ATF2 phosphorylation was observed.

Strikingly, both IL-8 and GM-CSF were found to be constitutively secreted from PTEN-deficient cells (Fig. 5*C*), and ATF activity has been associated with the transcription of both of these genes (18, 19). The level of IL-8 secretion was similar to that of FcεRI-stimulated control cells, whereas GM-CSF secretion was ~50% of the stimulated response. Thus, these genes appear to be highly dependent on PIP_3 production for their activation. This possibility was further explored by treatment of control or PTEN-deficient cells with the PI3K inhibitor wortmannin. Cytokine secretion from control cells was inhibited (ranging from 60 to 90%). However, wortmannin failed to block the constitutive or stimulated secretion of cytokines from the PTEN-deficient HuMCs. Thus, PTEN deficiency bypassed the need for FcεRI-stimulated PI3K activity.

SHIP-1 and −2 are present in PTEN-deficient cells, advancing the view that PTEN is key in the homeostatic control of PIP_3 levels. This hypothesis is consistent with the tumor suppressive properties of PTEN (7). Control of both Akt and MAP kinase basal activity by PTEN appears to be a vital function that governs the constitutive production of proinflammatory cytokines linked to tumor promotion (20). In FcεRI-initiated responses, PTEN appears to be contributory for PIP_3 regulation. However, the FcεRI-stimulated phenotype of SHIP-null mast cells is almost identical with that of FcεRI-stimulated PTEN-deficient mast cells (5), suggesting significant redundancy in the regulation of PIP_3 levels in stimulated cells. Of particular interest is whether PTEN function in homeostasis is entirely independent of cell stimulation (as suggested herein) and whether loss/decline of PTEN activity might alter mast cell function in health and disease.

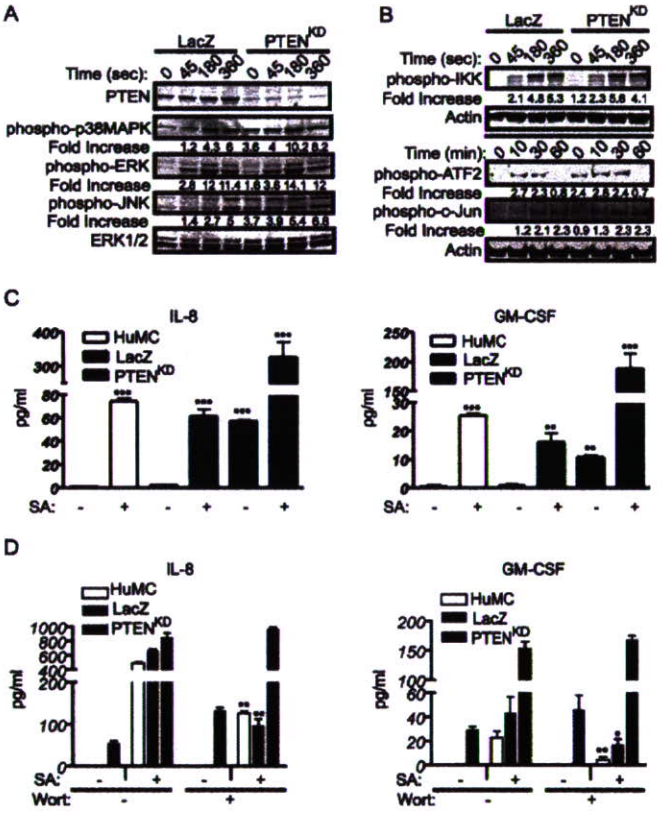

FIGURE 5. Constitutive and enhanced FcεRI-stimulated MAP kinase phosphorylation and cytokine secretion in PTEN-deficient human mast cells. *A*, Biotinylated IgE-sensitized HuMCs were stimulated or not stimulated with 100 ng/ml SA. The PTEN expression level and the phosphorylation of MAP kinases was determined with Abs to PTEN and to phosphorylated (phospho-) p38, ERK, and JNK. The ERK protein was used for normalization. Fold increase is normalized to nonstimulated LacZ control. *B*, PTEN-deficient HuMCs were stimulated and processed as described above for the indicated times. Phosphorylation of IKK, c-Jun, and ATF2 was detected by immunoblot with phosphorylated (phospho-) IKK, c-Jun, and ATF2 antibodies. Actin protein was used for loading control. One representative experiment of three is shown (*A* and *B*). *C*, PTEN-deficient HuMCs were stimulated as previously described (13). Secreted IL-8 and GM-CSF were measured by ELISA. Data are reported as mean ± SEM of three individual experiments. Significance is relative to wild-type cells (**, $p < 0.005$; ***, $p < 0.0005$). *D*, Experiments were conducted as in *C*, but 30 nM wortmannin (Wort., a PI3K inhibitor) was added to nonstimulated or FcεRI-stimulated cells for 60 min before stimulation. Cytokine secretion was measured as in *C*. Significance is relative to untreated cells (*, $p < 0.05$; **, $p < 0.005$; ***, $p < 0.0005$).

Disclosures

The authors have no financial conflict of interest.

References

1. Smith, A. J., Z. Surviladze, E. A. Gaudet, J. M. Backer, C. A. Mitchell, and B. S. Wilson. 2001. p110β and p110δ phosphatidylinositol 3-kinase up-regulate FcεRI-activated Ca^{2+} influx by enhancing inositol 1,4,5-trisphosphate production. *J. Biol. Chem.* 276: 17213–17220.
2. Gu, H., K. Saito, L. D. Klaman, J. Shen, T. Fleming, Y. Wang, J. C. Pratt, G. Lin, B. Lim, J. P. Kinet, and B. G. Neel. 2001. Essential role for Gab2 in the allergic response. *Nature* 412: 186–190.
3. Parravicini, V., M. Gadina, M. Kovarova, S. Odom, C. Gonzalez-Espinosa, Y. Furumoto, S. Saitoh, L. E. Samelson, J. J. O'Shea, and J. Rivera. 2002. Fyn kinase initiates complementary signals required for IgE-dependent mast cell degranulation. *Nat. Immunol.* 3: 741–748.
4. Ali, K., A. Bilancio, M. Thomas, W. Pearce, A. M. Gilfillan, C. Tkaczyk, N. Kuehn, A. Gray, J. Giddings, E. Peskett, et al. 2004. Essential role for the p110δ phosphoinositide 3-kinase in the allergic response. *Nature* 431: 1007–1011.
5. Huber, M., C. D. Helgason, J. E. Damen, L. Liu, R. K. Humphries, and G. Krystal. 1998. The src homology 2-containing inositol phosphatase (SHIP) is the gatekeeper of mast cell degranulation. *Proc. Natl. Acad. Sci. USA* 95: 11330–11335.
6. Odom, S., G. Gomez, M. Kovarova, Y. Furumoto, J. J. Ryan, H. V. Wright, C. Gonzalez-Espinosa, M. L. Hibbs, K. W. Harder, and J. Rivera. 2004. Negative regulation of immunoglobulin E-dependent allergic responses by Lyn kinase. *J. Exp. Med.* 199: 1491–1502.
7. Cantley, L. C., and B. G. Neel. 1999. New insights into tumor suppression: PTEN suppresses tumor formation by restraining the phosphoinositide 3-kinase/AKT pathway. *Proc. Natl. Acad. Sci. USA* 96: 4240–4245.
8. Di Cristofano, A., B. Pesce, C. Cordon-Cardo, and P. P. Pandolfi. 1998. Pten is essential for embryonic development and tumour suppression. *Nat. Genet* 19: 348–355.
9. Tkaczyk, C., M. A. Beaven, S. M. Brachman, D. D. Metcalfe, and A. M. Gilfillan. 2003. The phospholipase Cγ1-dependent pathway of FcεRI-mediated mast cell activation is regulated independently of phosphatidylinositol 3-kinase. *J. Biol. Chem.* 278: 48474–48484.

10. Gomez, G., C. Gonzalez-Espinosa, S. Odom, G. Baez, M. E. Cid, J. J. Ryan, and J. Rivera. 2005. Impaired FcεRI-dependent gene expression and defective eicosanoid and cytokine production as a consequence of Fyn-deficiency in mast cells. *J. Immunol.* 175: 7602–7610.
11. Nilsson, G., T. Blom, M. Kusche-Gullberg, L. Kjellen, J. H. Butterfield, C. Sundstrom, K. Nilsson, and L. Hellman. 1994. Phenotypic characterization of the human mast-cell line HMC-1. *Scand. J. Immunol.* 39: 489–498.
12. Tkaczyk, C., D. D. Metcalfe, and A. M. Gilfillan. 2002. Determination of protein phosphorylation in FcεRI-activated human mast cells by immunoblot analysis requires protein extraction under denaturing conditions. *J. Immunol. Methods* 268: 239–243.
13. Hundley, T. R., A. M. Gilfillan, C. Tkaczyk, M. V. Andrade, D. D. Metcalfe, and M. A. Beaven. 2004. Kit and FcεRI mediate unique and convergent signals for release of inflammatory mediators from human mast cells. *Blood* 104: 2410–2417.
14. Miyagishi, M., S. Matsumoto, and K. Taira. 2004. Generation of an shRNAi expression library against the whole human transcripts. *Virus Res.* 102: 117–124.
15. Downward, J. 2004. PI 3-kinase, Akt, and cell survival. *Semin. Cell Dev. Biol.* 15: 177–182.
16. Saitoh, S., S. Odom, G. Gomez, C. L. Sommers, H. A. Young, J. Rivera, and L. E. Samelson. 2003. The four distal tyrosines are required for LAT-dependent signaling in FcεRI-mediated mast cell activation. *J. Exp. Med.* 198: 831–843.
17. Karin, M. 1998. Mitogen-activated protein kinase cascades as regulators of stress responses. *Ann. NY Acad. Sci.* 851: 139–146.
18. Himes, S. R., L. S. Coles, R. Katsikeros, R. K. Lang, and M. F. Shannon. 1993. HTLV-1 tax activation of the GM-CSF and G-CSF promoters requires the interaction of NF-κB with other transcription factor families. *Oncogene* 8: 3189–3197.
19. Marin, V., C. Farnarier, S. Gres, S. Kaplanski, M. S. Su, C. A. Dinarello, and G. Kaplanski. 2001. The p38 mitogen-activated protein kinase pathway plays a critical role in thrombin-induced endothelial chemokine production and leukocyte recruitment. *Blood* 98: 667–673.
20. Lazar-Molnar, E., H. Hegyesi, S. Toth, and A. Falus. 2000. Autocrine and paracrine regulation by cytokines and growth factors in melanoma. *Cytokine* 12: 547–554.

Journal of Reproduction and Development, Vol. 52, No. 3, 2006

—Full Paper—

Down-Regulation of Endogenous *Wt1* Expression by *Sry* Transgene in the Murine Embryonic Mesonephros-Derived M15 Cell Line

Masanori ITO[1)], Makoto MIYAGISHI[1,2)], Chisato MURATA[1,3)], Hiroaki KAWASAKI[1,2)], Tadashi BABA[3)], Chikashi TACHI[1,4,5)] and Kazunari TAIRA[1,2)]

[1)]Gene Function Research Center, National Institute of Advanced Industrial Science and Technology (AIST), Central 4, 1–1–1 Higashi, Tsukuba Science City, Ibaraki 305-8562, [2)]Department of Chemistry and Biotechnology, School of Engineering, The University of Tokyo, Hongo, Tokyo 113-8656, [3)]Graduate School of Life and Environmental Sciences, University of Tsukuba, Tsukuba Science City, Ibaraki 305-8572, [4)]Laboratory of Reproductive and Developmental Biotechnology, Department of Animal Resource Sciences, School of Veterinary Medicine and Life Sciences, Azabu University, Sagamihara-shi 229-8501 and [5)]Mouse Genome Engineering Center, Mitsubishi-kagaku, Life Science Institute, Machida-shi, Tokyo 194-0031, Japan

Abstract. *Wt1* is one of numerous candidate genes comprising the hypothetical chain of gene expression essential for male sex differentiation of the bipotential indifferent gonads during embryogenesis. However, the evidence in the literature is ambivalent regarding the position of *Wt1* relative to *Sry* in this scheme; *Wt1* might act either upstream or downstream of *Sry*. In the present study, the effects of *Sry* expression upon *Wt1* were investigated using M15 cells (XX karyotype), which are derived from murine embryonic mesonephros and express endogenous *Wt1*. In 3 stably-transformed *Sry*-expressing M15 cell lines, we showed that the expression levels of the mRNAs coding for all 4 isoforms of the WT1 proteins were down-regulated. Similarly, *Wnt* 4 expression was down-regulated in these cell lines. Silencing of *Sry* in the transformed cell lines using ribozymes or short hairpin RNAs (shRNAs) resulted in elevated levels of *Wt1* and *Wnt4* expression. These results strongly indicate that *Wt1* might be under the control of *Sry* during gonadal differentiation in the mouse. In electrophoretic mobility shift assays (EMSA), we demonstrated that the 3.7 kb 5′-upstream DNA stretch of *Wt1* containing potential Sry binding sites was capable of forming molecular complexes with nuclear protein(s) from *Sry* expressing cells but not with those from control non-*Sry* expressing cells. In summary, our present results support the notion that *Wt1* is located downstream of *Sry* and down-regulated by the sex determining gene. Although the precise biological meaning of the present findings have yet to be clarified, it is possible that *Wt1* plays a dual role during gonadal differentiation, i. e., turning on *Sry* expression on one hand, and being down-regulated by its product, Sry, on the other, possibly forming a type of negative feed-back mechanism. Further work is needed to substantiate this view.

Key words: Sex determination, *Sry*, *Wt1*, shRNA, Ribozyme

(J. Reprod. Dev. 52: 415–427, 2006)

Accepted for publication: February 16, 2006
Published online: March 27, 2006
Correspondence: C. Tachi (e-mail: ch-tac@dol.hi-ho.ne.jp)

SRY (*Sry* in the mouse) [1, 2] is the 'master gene' for initiating male sex differentiation in the bipotential indifferent gonads of mammals [3]. The *Sry*-encoded protein, SRY (Sry in the mouse), possesses an HMG domain and acts as a transcription factor, triggering a cascade of gene expression, i.e., the *Sry* cascade [4, 5].

Numerous genes have been suggested in the literature as candidate genes comprising the hypothetical chain of gene expression essential for male differentiation of the primordial gonads during embryogenesis., e.g., *Wt1* [6–9], *Sf1/Ad4BP* [10–12], *Wnt4* [13], *Amh* (*MIS*) [14, 15] and *Sox9* [16–18] among many others (see [19, 20] for recent reviews).

As a part of our effort to experimentally identify the target genes of Sry action, we introduced an *Sry* expression vector driven by CMV promoter into a non-*Sry* expressing TM-4 cell line derived from cultured mouse Sertoli cells [21], and a mouse ES cell line with the XX karyotype, TMA-18 [8]. In the TMA-18 cells, the *Sry* transgene stably incorporated into their genomes induced expression of endogenous *Wt1* [8]. On the other hand, in TM-4 cells, the *Sry* transgene induced expression of endogenous *Cyp19a1* (synonimous to *P-450arom*), and *Wt1* expression was not induced in these cells.

These results suggested that the effects of *Sry* expression might vary according to the differentiation status of the cells and that the appropriate combinations of cells of different differentiation statuses and *Sry* transgene could give us clues toward understanding the molecular mechanisms underlying sex differentiation in the mouse.

It has been shown that *WT1* is expressed in the lateral mesenchyme and that it is involved in genitourinary development in humans [22]. Subsequently it was demonstrated in the mouse that *Wt1* is expressed from 9.0 dpc [23] before the onset of the surge of Sry expression, i. e., 10.5 dpc [24]. It was hypothesized, therefore, that *Wt1* might be located upstream, rather than downstream, of *Sry* in the chain of gene expression leading to sexual differentiation of the primordial gonads in the mouse. Concomitantly, on the other hand, it has also been shown that the *Wt1* promoter contains a consensus DNA binding sequence for Sry [25], suggesting the possibility that *Wt1* might be regulated by *Sry*.

Human *WT1* expression vector constructs transfected into 3 different types of cultured cell lines, i. e., murine TM4, human HeLa, and human NT2D1, either transiently or stably have been shown to be capable of activating the promoter of the co-transfected full-length human *SRY* DNA construct [26]. However, the WT1 binding site present in the human *SRY* promoter is not conserved in the mouse [26], raising a question about simple generalization of the findings made in the human *WT1-SRY* system to the murine equivalent.

A mouse mesonephric cell line with the XX karyotype, M15, has been known to express high levels of the 4 wild-type WT1 protein isoforms, i. e., with or without the 17 amino acids encoded by exon 5 (+ or –exon 5) and with or without KTS (+ or –KTS) between the 3rd and 4th zinc fingers [27]. It should serve, therefore, as an appropriate cell line for investigation of the effects of *Sry* expression on the endogenous expression of *Wt1*. In the present study, we attempted to examine the effects of *Sry* expression upon the endogenous expression of *Wt1* in M15 cells by employing ribozyme and RNAi technology to inactivate the *Sry* transcripts.

Materials and Methods

Cell culture

The M15 cell line (XX karyotype) originally derived from mesonephric epithelial cells of the mouse embryo [27] was kindly provided by Dr. T. Noce, Mitsubishi-kagaku Life Science Institute, Machida-shi, Tokyo, Japan. The cells were cultured in Dullbecco's Modified Eagle's Medium (DMEM; Sigma, St. Louis, MO, USA) containing heat inactivated FBS [10% (v/v); Gibco, Rockville, MD], penicillin (10,000 U/l; Sigma), and streptomycin (10 mg/l; Sigma) (this medium will be referred to as DMEM/10 below) under a humidified atmosphere of 5% CO_2 in air at 37 C.

Transfection of plasmids

Plasmids were transfected to the cell cultures using PolyFect Reagent (Qiagen, Valencia, CA, USA) according to manufacturer's instructions. For establishment of stably transformed cell lines, cells transfected with linearized plasmids were cultured for 48 h in DMEM/10. Then, the medium was changed to fresh DMEM/10 containing G418 (500 mg/ml; Sigma) and the cells were cultured for an

Table 1. List of primer sets used for the analysis of the effects of *Sry* transgene upon the expression of putative cascade genes in M15 cells

Genes	Primer sets	Sequences	Annealing temperature	Size of products
Sry	Sry-F Sry-R	5′-GGGACTGGTGACAATTGTCT-3′ 5′-ATCAACAGGCTGCCAATAAA-3′	56 C	440 bp
Wt1++	Wt1-F exon5+ Wt1-R KTS+	5′-GCTGGGAGCTCCAGCTCAGT-3′ 5′-GGGCTTTTCACTTGTTTTAC-3′	56 C	488 bp
Wt1+-	Wt1-F exon5+ Wt1-R KTS-	5′-GCTGGGAGCTCCAGCTCAGT-3′ 5′-GAAGGGCTTTTCACCTGTATGA-3′	56 C	482 bp
Wt1-+	Wt1-F exon5- Wt1-R KTS+	5′-TACCTTAAAGGGCCACGGTAT-3′ 5′-GGGCTTTTCACTTGTTTTAC-3′	56 C	456 bp
Wt1--	Wt1-F exon5- Wt1-R KTS-	5′-TACCTTAAAGGGCCACGGTAT-3′ 5′-GAAGGGCTTTTCACCTGTATGA-3′	56 C	450 bp
Wnt4	Wnt4-F Wnt4-R	5′-ACGGCACCATGAGCCCCCGTTC-3′ 5′-AGGCCACACCTGCTGAAGAG-3′	56 C	374bp
Sox9	Sox9-F Sox9-R	5′-GTGGCAAGTATTGGTCAA-3′ 5′-GAACAGACTCACATCTCT-3′	50 C	321 bp
Gata4	Gata4-F Gata4-R	5′-ATCAACCGGCCCCTCATTAAG-3′ 5′-GACAGCTTCAGAGCAGACAGC-3′	58 C	472 bp
Sf1	Sf1-F Sf1-R	5′-TGGTGTCCAGTGTCCACCCTTAT-3′ 5′-TCCGTGCACGTGTAATGCTTGT-3′	60 C	212 bp
Amh	AMH-F AMH-R	5′-TCCTACATCTGGCTGAAGTGATATGGGAGC-3′ 5′-CTCAGGGTGGCACCTTCTCTGCTTGGTTGA-3′	65 C	276 bp
Atrx	Atrx-F Atrx-R	5′-AGCAGATGATGGTGAACTCCG-3′ 5′-GTGTCTTCTGAATCCTCACTG-3′	56 C	236 bp
Hprt	Hprt-F Hprt-R	5′-GAAAGACTTGCTCGAGATGTCATG-3′ 5′-TGGCAACATCAACAGGACTCCTCG-3′	56 C	570 bp

additional 10 days. The surviving cell colonies were randomly picked up, expanded in fresh DMEM/10, and established as stably transformed cell lines. Cellular proliferation rates were determined using a CellTiter-Glo Luminescent Cell Viability Assay kit (Promega, Madison, WI, USA).

Reverse transcriptase mediated polymerase chain reaction (RT-PCR)

Two micrograms of total RNA isolated from the cell cultures using Isogen (Wako, Osaka, Japan) were heat-denatured and reverse-transcribed into cDNA using M-MLV Reverse Transcriptase (Promega). The primer pairs used for PCR amplification of the DNA sequences of the relevant target genes are listed in Table 1. The optimal conditions for PCR amplification were determined for each primer pair prior to the experiments. The size of the target amplicons was confirmed by electrophoresis of the PCR products on 2% agarose gels in TAE buffer. Densitometric analysis of the electrophoretograms was conducted using NIH ImageJ (NIH, Bethesda, MD, USA; http://rsb.info.nih.gov/ij/).

Expression vector constructs

Sry and *Wnt4*: The *Sry* expression vector used in the present series of experiments, pCMV/mSry, was described previously [8, 21]. An empty vector for the control mock-transformation experiments was constructed by removing the *Sry* coding region from pCMV/mSry by *XbaI* digestion and self-ligating the linearized plasmid. *Wnt4* cDNA was generated by reverse transcription of the total RNA extracted from the gonads of C57BL/6J female mice on 13.5 dpc as described previously [28] and was PCR-amplified using the primer pair 5′-ACG-GCA-CCA-TGA-GCC-CCC-GTT-C-3′ (forward) and 5′-TCA-CCG-GCA-CGT-GTG-CAT-CTC-C-3′ (reverse). The 1 kb segment of *Wnt4* cDNA

Table 2. List of sense strand DNA sequences for shRNA targeted to *Sry* (see text for details)

Name	Sense strand DNA sequences for shRNA	Target site*
tRNA-shRNA1	TACAACCTTCTGCAGTGGGAtAGGAAttGAAAAGGG TTCCTGTCCCACTGCAGAAGGTGTA	295–323
tRNA-shRNA2	TACAGGCAAGACTGGAGTAGAGtTGtAtAGAAAATGT GCAGCTCTACTCCAGTCTTGCCTGTA	337–365
tRNA-shRNA3	CCTGTTGATATCCCtAtTGGGtACttGtAGAAAATGCAGGT GCCCAGTGGGGATATCAACAGG	403–431
tRNA-shRNA4	TACTTACTAACAGCTGAtATCAtTGGTGAGAAAATCACC AGTGATGTCAGCTGTTAGTAAGTA	1105–1133
tRNA-shRNA5	ATCACTGGTGAGCATAtAttAUAttAGGAGAAAATCCTGG TATGGTGTATGCTCACCAGTGAT	1123–1151
tRNA-shRNA6	ATACACCATACCAGGAGtAtCTtAGtAtAGAAAATGTGCT GAGGTGCTCCTGGTATGGTGTAT	1136–1164
tRNA-shRNA7	CACCTCAGCACAGCCtTGTGGTTGGtAGTGAAAAACTG CCAACCACAGGGCTGTGCTGAGGTG	1153–1181
tRNA-shRNA8	GCACAGCCCTGTGGTTGGtAGTCTtATGAGAAAATCAT GAGACTGCCAACCACAGGGCTGTGC	1160–1188
U6-shRNA1	GCAtAGAGgTTGAAGgTCAACGTGTGCTGTCCGTTGAT CTTCAATCTCTGTGCTTTTT	172–190
U6-shRNA2	GATTGgAGATtCTAtACAAACGTGTGCTGTCCGTTTGTG TAGGATCTTCAATCTTTTT	179–197
U6-shRNA3	AGgGAAATAtCCAAAtTATACGTGTGCTGTCCGTATAGT TTGGGTATTTCTCTTTTTT	198–216
U6-shRNA4	GAGgAATAtCCAAAtTATAACGTGTGCTGTCCGTTATAG TTTGGGTATTTCTCTTTTT	199–217
U6-shRNA5	ACtCAAAtTATAAATgTCAACGTGTGCTGTCCGTTGATAT TTATAGTTTGGGTTTTTT	206–224
U6-shRNA6	GGtTAAAGTGTtACgGAGAACGTGTGCTGTCCGTTCTCT GTGACACTTTAGCCTTTTT	237–255
U6-shRNA7	ACgGGAACtCACATGtCATACGTGTGCTGTCCGTATGGC ATGTGGGTTCCTGTTTTTT	314–332
U6-shRNA8	GCgGCAGtATCAGTTtCATACGTGTGCTGTCCGTATGGA ACTGATGCTGCTGCTTTTT	828–846

* The base numbers indicate the target sites in the coding region of *Sry* (NM_011564).

obtained was inserted into pGEM-T Easy vector (Promega). To obtain a mammalian expression vector for *Wnt4* (pCX-Wnt4) the *Eco*RI/*Eco*RI fragment of *Wnt4* cDNA (Fig. 4) was inserted into pCX-blank, which was made by removing the EGFP sequence from pCX-EGFP [29] (kindly provided by Dr. M. Okabe, Osaka University, Osaka, Japan) by *Eco*RI restriction. Similarly, the mammalian expression vector for *Sry*, pCX-Sry, was constructed by inserting the blunted *Xba*I/*Spe*I fragment of the *Sry* coding region into a blunted linearized pCX-blank. Because pCX-Sry has an artificial intron, the primer set for RT-PCR amplification of the transcript was positioned so that they contained the intron as a marker specific to the transcript; the primer pair used consisted of 5′-CTG-ACC-GCG-TTA-CTC-CCA-CA-3′ (forward) and 5′-GGT-ATT-TCT-CTC-TGT-GTA-GG-3′ (reverse).

tRNA-ribozyme complexes: Vectors for expression of tRNA-ribozyme complexes targeted to *Sry* was constructed using pPUR-tRNA plasmid [30], which includes a promoter for the human $tRNA^{Val}$ gene between the *Eco*RI and *Bam*HI sites of pPUR